

Scan B -Statistic for Kernel Change-Point Detection

Shuang Li

SLI370@GATECH.EDU

*H. Milton Stewart School of Industrial and Systems Engineering
Georgia Institute of Technology
Atlanta, GA 30332, USA*

Yao Xie (corresponding author)

YAO.XIE@ISYE.GATECH.EDU

*H. Milton Stewart School of Industrial and Systems Engineering
Georgia Institute of Technology
Atlanta, GA 30332, USA*

Hanjun Dai

HANJUNDAI@GATECH.EDU

*College of Computing
Georgia Institute of Technology
Atlanta, GA 30332, USA*

Le Song

LSONG@CC.GATECH.EDU

*College of Computing
Georgia Institute of Technology
Atlanta, GA 30332, USA*

Editor:

Abstract

Detecting the emergence of an abrupt change-point is a classic problem in statistics and machine learning. Kernel-based nonparametric statistics have been used for this task which enjoy fewer assumptions on the distributions than the parametric approach and can handle high-dimensional data. In this paper we focus on the scenario when the amount of background data is large, and propose two related computationally efficient kernel-based statistics for change-point detection, which are inspired by the recently developed B -statistics. A novel theoretical result of the paper is the characterization of the tail probability of these statistics using the change-of-measure technique, which focuses on characterizing the tail of the detection statistics rather than obtaining its asymptotic distribution under the null distribution. Such approximations are crucial to control the false alarm rate, which corresponds to the significance level in offline change-point detection and the average-run-length in online change-point detection. Our approximations are shown to be highly accurate. Thus, they provide a convenient way to find detection thresholds for both offline and online cases without the need to resort to the more expensive simulations or bootstrapping. We show that our methods perform well on both synthetic data and real data.

Keywords: Change-Point Detection, Kernel-Based Tests, Online Algorithm, Tail Probability, False-Alarm Control.

1. Introduction

Given a sequence of samples, x_1, x_2, \dots, x_t , from a domain \mathcal{X} , we are interested in detecting a possible change-point τ , such that before the change samples x_i are *i.i.d.* with a null

distribution P , and after the change samples x_i are *i.i.d.* with a distribution Q . Here, the time horizon t is either fixed, $t = T_0$, which we call the offline or fixed-sample change-point detection, or t is not fixed, meaning that one can keep getting new samples, which we call the online or sequential change-point detection. In the offline setting, our goal is to detect the existence of a change. In the online setting, our goal is to detect the emergence of a change as soon as possible after it occurs. Here, we restrict our attention to detecting one change-point. One such instance is seismic event detection (Ross and Ben-Zion, 2014), where we would like to either detect the presence of a weak event in retrospect to better understand the geophysical structure or detect the event as quickly as possible for online monitoring.

Ideally, the detection algorithm should be free of distributional assumptions to be robust when applied to real data. To achieve this goal, various kernel based statistics have been proposed in the machine learning literature (Harchaoui et al., 2008; Enikeeva and Harchaoui, 2014; Zou et al., 2014b; Kifer et al., 2004; Song et al., 2013; Desobry et al., 2005), which are suitable for vector observations and typically work better in real data. Kernel approaches are distribution free and more robust as they provide consistent results over larger classes of data distributions; albeit they can be less powerful in settings where a clear distributional assumption can be made. However, most kernel based statistics cost $\mathcal{O}(n^2)$ to compute over n samples. In online change-point detection, the number of samples grows with time and hence we cannot directly use the naive approach. Recently, Zaremba et al. (2013) develop the so-called B -test statistic to reduce the computational complexity. The B -test statistic samples N pairs of blocks of size B from the two-sample data, compute the unbiased estimates of the kernel-based statistic between each pair, and then taken an average. The computational complexity of the B -statistics reduces to $\mathcal{O}(BN^2)$ or equivalently $\mathcal{O}(Nn)$ instead of $\mathcal{O}(n^2)$.

In this paper, we present two related scan B -statistics for change-point detection. The proposed statistics are based on kernel maximum mean discrepancy (MMD) (Gretton et al., 2012; Harchaoui et al., 2013). Our methods are inspired by the B -statistic but differ in various ways to tailor to the need of change-point detection. Typically, there is a small number of post-change samples (for instance, seismic events are relatively rare, and in online change-point detection, one would like to detect the change quickly). But there is a large amount of reference data. So when constructing the detection statistic, we reuse the post-change samples for the test block, but construct multiple and disjoint reference blocks. This leads to non-negligible dependence between the MMD statistics being averaged over and we cannot use the approach in existing works to analyze them. Moreover, the scanning nature of the proposed statistic also introduces non-negligible dependence. We construct the reference and test blocks in a structured way, so that analytical expressions can be obtained when analyzing the false alarm rates.

Our main theoretical contribution includes accurate theoretical approximations to the false-alarm rate of scan B -statistics. Controlling false alarms is a key challenge in change-point detection. Specifically, this means to quantify the significance level for offline change-point detection, and the average run length (ARL) for online change-point detection. We cannot directly use the null property of the B -statistic from the existing work, because the scan statistics take the maximum of multiple B -statistics computed over highly overlapping data blocks. Due to such strong correlations, one cannot use the central limit theorem or

even the martingale central limit theorem as used by existing work. Instead, we adopt a recently developed change-of-measure technique (see, *e.g.*, Yakir (2013)) for scan statistics, which are capable of dealing with the more challenging situation here. Such a technique is quite general, although it has not been used much in the machine learning community.

Our contribution also includes: (1) obtaining a closed-form variance estimator, which allows easy calculation of the B -statistics; (2) further improving the accuracy of our approximations by taking into account the skewness of the kernel-based statistics. The accuracy of our approximations is validated by numerical examples. Finally, we demonstrate the good performance of our method using real speech and human activity data.

1.1 Related work

Classic parametric approaches for change-point detection can be found in Siegmund (1985); Tartakovsky et al. (2014). There has been an array of nonparametric change-point detection methods. Notable non-parametric schemes for change-point detection include Gordon and Pollak (1994); Picard (1985), which are designed for scalar observations and not suitable for vector observations. Brodsky and Darkhovsky (2013) provide a comprehensive introduction to the methodologies and applications of nonparametric change-point detection. Bibinger et al. (2017) construct a nonparametric minimax-optimal test to discriminate continuous paths with volatility jumps and prove weak convergence of the test statistic to an extreme value distribution. In the online setting, Kifer et al. (2004) present a meta-algorithm which compares data in some “reference window” to the data in the current window, using empirical distance measures that are not kernel-based; Desobry et al. (2005) detect abrupt changes by comparing two sets of descriptors extracted online from the signal at each time instant: the immediate past set and the immediate future set, and then use a soft margin single-class support vector machine to build a dissimilarity measure (which is asymptotically equivalent to the Fisher ratio in the Gaussian case) in the feature space between those sets without estimating densities as an intermediate step; Song et al. (2013) present a density-ratio estimation method to detect change-points, fitting the density-ratio using a non-parametric Gaussian kernel model, whose parameters are updated online via stochastic gradient descent approach. Another important branch of nonparametric change-point detection method is based on Kolmogorov-Smirnov test (Jr, 1951; Lilliefors, 1967), which has been used in biostatistics (Wilcox, 2005; Wang et al., 2014; Wan et al., 2014). The generalization of Kolmogorov-Smirnov test from the univariate setting to the multi-dimensional setting is given by the Peacock’s test (Fasano and Franceschini, 1987), which, however, is less convenient to use than the kernel-based statistic test.

Seminal works by Csörgő and Horváth (1988) studied kernel-based U -statistic for the change-point detection. They show that the statistic indexed by the assumed change-point location parameter k , after proper standardization and rescaling of time and magnitude, converges in distribution to a Gaussian process under the null, and converges to a deterministic path in probability under the alternative, when the number of samples goes to infinity. These results are useful for bounding the detection statistics under the null with high-probability (hence, controlling the false detection), and for studying the consistency of tests. Csörgő and Horváth (1997) and Serfling (2009) contain comprehensive discussions on asymptotic theory of non-parametric statistics including U -statistics. Our scan B -statistic

can also be viewed as a form of U -statistic using appropriate definition of the kernel. The main differences of these classic work from our proposed B -statistic are: (1) our statistic uses B -test block decomposition and averaging to make the test statistic more computationally efficient; (2) our statistic is more challenging to analyze due to the block structure and correlation introduced by scanning statistics; (3) our analytical approach is different: Csörgő and Horváth (1988) leverage invariance principle to establish convergence of the entire sample path; we focus on characterizing the tail probability of the statistic under the null and use the change-of-measure technique to achieve good approximation accuracy.

Other existing works that also focus on establishing asymptotic distribution of the detection statistic under the null for controlling the false alarm rate including the following: Harchaoui et al. (2008) present a maximum kernel Fisher discriminant ratio statistic and study its asymptotic null distribution; Dehling et al. (2015) investigate the two-sample test U -statistic for dependent data. Our approach is different from above, in that we focus on directly approximating the tail of the detection statistic under the null, rather than trying to obtain its asymptotic distribution. Moreover, traditional analyses are usually done for offline change-point detection, while our analytical framework based on change-of-measure can be applied to both offline and online change-point detection.

Change-point detection problems are related to the classical statistical two-sample test. However, they are usually more challenging than two-sample test because the change-point location τ is unknown. Hence, when forming the detection statistic, one has to “taking the maximum” of the detection statistics. The statistic being maxed over are usually highly correlated since they are computed using overlapping data. Hence, when analyzing the false detection rate, more sophisticated probabilistic tools have to be used.

Our techniques for approximating false alarm rates differ from large-deviation techniques (see, e.g., Dembo and Zeitouni (2009)), which establish exponential rate by which the probability converges to zero. In certain scenarios, the first-order approximation obtained from large-deviation technique may not be sufficient for choosing threshold. Our method provides more refined approximations to include polynomial terms and constants.

Finally, there are also works taking different approaches than hypothesis test for change-point detection. For instance, Harchaoui and Cappé (2007) develop a kernel-based multiple-change-point detection approach, where the optimal location to segment the data is obtained by dynamic programming; Arlot et al. (2012) treat multiple change-point detection as an estimation problem, develop a kernelized linear model and provide a non-asymptotic oracle inequality for the estimation error. In the offline setting, Zou et al. (2014b) study a problem when there are s anomalous sequences out of n sequences to be detected, and the test statistic is constructed using MMD; Matteson and James (2014) propose a non-parametric approach based on U -statistics, which is capable of consistently estimating an unknown number of multiple change-point locations; Zou et al. (2014a) propose a non-parametric maximum likelihood approach, with the number of change-points determined from the Bayesian information criterion (BIC) and the locations of the change-points are estimated via dynamic programming

Our notations are standard. Let I_k denote the identity matrix of size k -by- k ; $[1, N] = \{1, 2, \dots, N\}$. Let $\mathbb{E}[A; \mathcal{B}] = \mathbb{E}[\mathcal{A}\mathbf{1}_{\mathcal{B}}]$ denote the expectation conditioned on event \mathcal{B} , where $\mathbf{1}_{\mathcal{B}}$ represents the indicator function that takes value 1 when the event \mathcal{B} happens and takes value 0, otherwise. Let $\text{Var}(\cdot)$ and $\text{Cov}(\cdot)$ denote the variance and the covariance. Let $\mathbf{0}$ and

\mathbf{e} denote vectors of all zeros and all ones, respectively. Let $[\Sigma]_{ij}$ denote the ij -th element of a matrix Σ . In Section 4, \mathbb{E}_B , Var_B , and Cov_B denote the values computed under the distribution after the change-of-measure. Similarly, in Section 5, \mathbb{E}_t , Var_t , and Cov_t denote the values obtained under the distribution after the change-of-measure.

2. Background

We briefly review kernel-based statistics and the maximum mean discrepancy. A reproducing kernel Hilbert space (RKHS) \mathcal{F} on \mathcal{X} with a kernel $k(x, x')$ is a Hilbert space of functions $f(\cdot) : \mathcal{X} \mapsto \mathbb{R}$ with inner product $\langle \cdot, \cdot \rangle_{\mathcal{F}}$. Its element $k(x, \cdot)$ satisfies the reproducing property: $\langle f(\cdot), k(x, \cdot) \rangle_{\mathcal{F}} = f(x)$, and consequently, $\langle k(x, \cdot), k(x', \cdot) \rangle_{\mathcal{F}} = k(x, x')$, meaning that we can view the evaluation of a function f at any point $x \in \mathcal{X}$ as an inner product. Commonly used RKHS kernel functions include Gaussian radial basis function (RBF) kernel $k(x, x') = \exp(-\|x - x'\|^2 / 2\sigma^2)$ where $\sigma > 0$ is the kernel bandwidth, and polynomial kernel $k(x, x') = (\langle x, x' \rangle + a)^d$ where $a > 0$ and $d \in \mathbb{N}$ (Schölkopf and Smola, 2002). RKHS kernels can also be defined for sequences, graph and other structured object (Schölkopf et al., 2004). In this paper, if not otherwise stated, we will assume that Gaussian RBF kernel is used.

Assume there are two sets, each containing n samples, each taking value on a general domain \mathcal{X} , where $X = \{x_1, x_2, \dots, x_n\}$ are *i.i.d.* with a distribution P , and $Y = \{y_1, y_2, \dots, y_n\}$ are *i.i.d.* with a distribution Q . The *maximum mean discrepancy* (MMD) is defined as (Gretton et al., 2012)

$$\text{MMD}[\mathcal{F}, P, Q] := \sup_{f \in \mathcal{F}} \{ \mathbb{E}_{X \sim P}[f(X)] - \mathbb{E}_{Y \sim Q}[f(Y)] \}.$$

An unbiased estimator of MMD^2 can be obtained using U -statistic (Gretton et al., 2012)

$$\text{MMD}_u^2[\mathcal{F}, X, Y] = \frac{1}{n(n-1)} \sum_{i, j \in [1, n], i \neq j} h(x_i, x_j, y_i, y_j), \quad (1)$$

where $h(\cdot)$ is the kernel for U -statistic, defined in terms of an RKHS kernel as

$$h(x_i, x_j, y_i, y_j) = k(x_i, x_j) + k(y_i, y_j) - k(x_i, y_j) - k(x_j, y_i). \quad (2)$$

Intuitively, the empirical test statistic MMD_u^2 is expected to be small (close to zero) if $P = Q$, and large if P and Q are far apart. The complexity for evaluating MMD_u^2 is $\mathcal{O}(n^2)$, since we have to form the so-called Gram matrix for the data, which is of size n -by- n . Under the null hypothesis, $P = Q$, the U -statistic is degenerate and has the same distribution as an infinite sum of Chi-square variables.

To improve computational efficiency, recently, an alternative approach to estimate MMD^2 has been proposed (called the B -test by (Zaremba et al., 2013)), which we refer to as the B -statistic in the following. The key idea is to partition the n samples from P and Q into N non-overlapping blocks, X_1, \dots, X_N and Y_1, \dots, Y_N , each of size B . Then compute $\text{MMD}_u^2[\mathcal{F}, X_i, Y_i]$ for each pair of blocks and then take the average:

$$\text{MMD}_B^2[\mathcal{F}, X, Y] = \frac{1}{N} \sum_{i=1}^N \text{MMD}_u^2[\mathcal{F}, X_i, Y_i].$$

Since B is constant and N is on the order of $\mathcal{O}(n)$, the computational complexity of $\text{MMD}_B^2[\mathcal{F}, X, Y]$ is $\mathcal{O}(B^2n)$, which is significantly lower than the $\mathcal{O}(n^2)$ complexity of $\text{MMD}_u^2[\mathcal{F}, X, Y]$. Furthermore, by averaging $\text{MMD}_u^2[\mathcal{F}, X_i, Y_i]$ over blocks, when the blocks are independent, the B -statistic is asymptotically normal under the null due to central limit theorem. This property allows a simple threshold to be derived for the B-test.

3. Scan B -statistic in change-point detection

Now we present our scan B -statistic based change-point detection schemes. Given a sequence of data $\{\dots, x_{-2}, x_{-1}, x_0, x_1, \dots, x_t\}$, each taking value on a general domain \mathcal{X} . Let $\{\dots, x_{-2}, x_{-1}, x_0\}$ denote the reference data that we know to follow the pre-change distribution, and there is a large amount of reference data is available.

In offline change-point detection, the number of samples is fixed and our goal is to detect the *existence* of a change-point τ , such that before the change-point, the samples are *i.i.d.* with a distribution P , and after the change-point, the samples are *i.i.d.* with a different distribution Q . The location τ where the change-point occurs is unknown. In other words, we are concerned with testing the null hypothesis

$$H_0 : x_i \sim P, \quad i = 1, \dots, t,$$

against the single change-point alternative

$$H_1 : \exists 1 \leq \tau < t \quad x_i \sim \begin{cases} Q, & i > \tau \\ P, & \text{otherwise.} \end{cases}$$

Note that we are interested in the case of a sustained change: before the change, all samples follow one distribution, and after the change, all samples follow another distribution and never switch back. In online change-point detection, the number of samples is not fixed, and we keep getting new samples; the goal is to detect the *emergence* of a change-point. In various change-point detection settings, the number of post-change samples is small, but the number of reference samples is large. Therefore, when constructing MMD statistics over blocks, we will use a common post-change block, and multiple disjoint pre-change reference blocks.

3.1 Offline change-point detection

For each possible change location τ , the post-change block Y consists of the most recent samples indexed from τ to t . Since we do not know the change-point location, we consider all possible meaningful τ values. This corresponds to considering a range of post-change block sizes B ranging from 2 (i.e., the most recent 2 samples are post-change samples; we exclude $B = 1$ because the corresponding procedure is very unstable) to B_{\max} .

The detection statistic is constructed as follows, as illustrated in Fig. 1(a). Data are split into $(N + 1)$ blocks of size B_{\max} . Treat the last block as the post-change block, and the remaining N blocks as reference data. Then we sample data from each block to form smaller sub-blocks of various size B , $B \in [2, B_{\max}]$. The reference blocks are denoted as $X_i^{(B)}$, $i = 1, \dots, N$, and the test block as $Y^{(B)}$. We compute MMD_u^2 for each reference

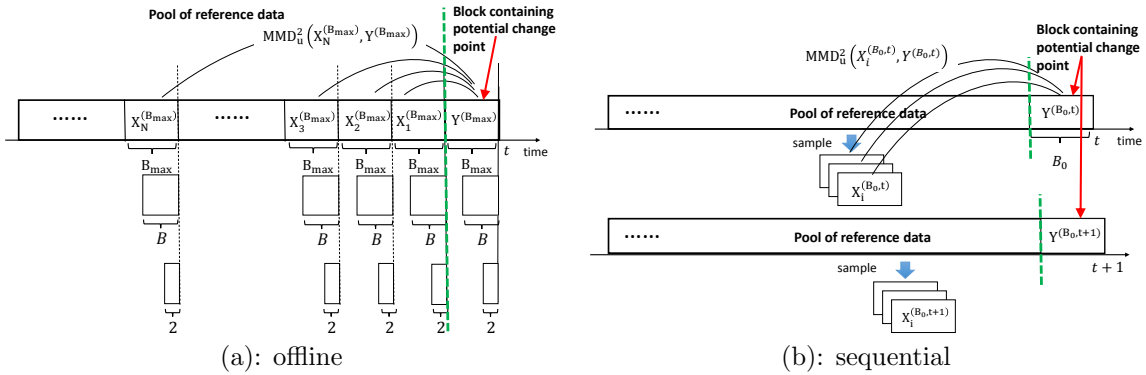


Figure 1: Illustration of (a) offline change-point detection: data are initially split into blocks of size B_{\max} ; then one samples from each initial block to form smaller blocks of various size B , $B = 2, \dots, B_{\max}$; (b) online change-point detection: the most recent B_0 samples form the test block, which is constantly updated with new data; the reference blocks of the same size B_0 are sampled from the reference pool of data.

sub-block with respect to the *common* post-change block, and take an average:

$$Z_B = \frac{1}{N} \sum_{i=1}^N \text{MMD}_u^2(X_i^{(B)}, Y^{(B)}). \quad (3)$$

Since the estimator MMD_u^2 is unbiased, under the null hypothesis $P = Q$, $\mathbb{E}[Z_B] = 0$. Let $\text{Var}[Z_B]$ denote the variance of Z_B under the null. The variance of Z_B depends on the block size B and the number of blocks N . Hence, we divide each Z_B by their standard deviation

$$Z'_B = Z_B / (\text{Var}[Z_B])^{1/2},$$

and take the maximum over all B to form the *offline B -statistic*. The variance $\text{Var}[Z_B]$ is given in Lemma 1, which facilitates its computation. A change-point is detected whenever the offline B -statistic exceeds a pre-specified threshold b :

$$\max_{2 \leq B \leq B_{\max}} Z'_B > b. \quad \{\text{offline change-point detection}\} \quad (4)$$

3.2 Online change-point detection

In the online setting, new samples arrive in a streaming fashion and we constantly test whether the incoming samples come from a different distribution. To reduce computational burden, in the online setting, we fix the block-size and adopt a *sliding window* approach.

The detection statistic is constructed as follows, as illustrated in Fig. 1(b). At each time t , we treat the most recent B_0 samples as the post-change block. Since in online change-point detection, we want to detect the change as quickly as possible, and hence typically there are not many post-change samples. There is large amount of reference data. To utilize data efficiently, we compare a common test block consisting of the most recent samples, with N different reference blocks. The reference blocks are formed by taking

NB_0 samples without replacement from the reference pool. Compute MMD_u^2 between each reference block with respect to the post-change block, and take an average:

$$Z_{B_0,t} = \frac{1}{N} \sum_{i=1}^N \text{MMD}_u^2(X_i^{(B_0,t)}, Y^{(B_0,t)}), \quad (5)$$

where B_0 is the fixed block-size, $X_i^{(B_0,t)}$ is the i -th reference block at time t , and $Y^{(B_0,t)}$ is the the post-change block at time t . When there is a new sample, we append it to the post-change block and purge the oldest sample. We show later that this construction allows for an explicit characterization of the false-alarm rate. We divide each statistic by its standard deviation to form the *online B-statistic*:

$$Z'_{B_0,t} = Z_{B_0,t} / (\text{Var}[Z_{B_0,t}])^{1/2}.$$

The calculation of $\text{Var}[Z_{B_0,t}]$ can also be achieved using Lemma 1. The online change-point detection procedure is a stopping time: an alarm is fired whenever the standardized detection statistic exceeds a pre-specified threshold $b > 0$:

$$T = \inf\{t : Z'_{B_0,t} > b\}. \quad \{\text{online change-point detection}\} \quad (6)$$

The online B -statistic can be computed efficiently. Note that the variance of the $Z_{B_0,t}$ only depends on the block size B_0 but independent of t . Hence, it can be pre-computed. Moreover, there is a simple recursive implementation of the online B statistic, with more details specified in Appendix A.

3.3 Analytical expression for $\text{Var}[Z_B]$

We obtain an analytical expression for $\text{Var}[Z_B]$, which is useful when forming the detection statistic in (4) and (6).

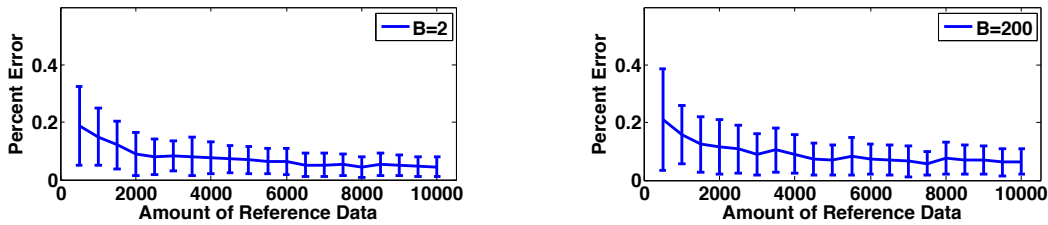
Lemma 1 (Variance of Z_B under the null) *Given a fixed block size $B \geq 2$ and number of blocks N , under the null hypothesis,*

$$\text{Var}[Z_B] = \binom{B}{2}^{-1} \left(\frac{1}{N} \mathbb{E}[h^2(x, x', y, y')] + \frac{N-1}{N} \text{Cov}[h(x, x', y, y'), h(x'', x''', y, y')] \right), \quad (7)$$

where x, x', x'', x''', y , and y' are i.i.d. random variables with the null distribution P .

The lemma is proved by making a connection between MMD_u^2 and U -statistic (Serfling, 1980) and utilizing the properties of U -statistic. Detail proof is provided in Appendix B. We verified numerically that Lemma 1 is quite accurate, as shown in Fig. 2.

Lemma 1 provides a much simpler way to estimate $\text{Var}[Z_B]$ than direct Monte Carlo simulation. When using direct Monte Carlo simulation, to generate 10000 instances of Z_B , one needs a total of $10000(N+1)B$ samples. Each Z_B needs $(N+1)B$ samples and is computationally expensive to evaluate. Using Lemma 1, one only needs to evaluate terms such as $\mathbb{E}[h^2(x, x', y, y')]$ and $\text{Cov}[h(x, x', y, y'), h(x'', x''', y, y')]$, which requires much fewer samples to achieve a good estimation accuracy.



(e): $B = 2$, % error for estimated variance (f): $B = 200$, % error for estimated variance

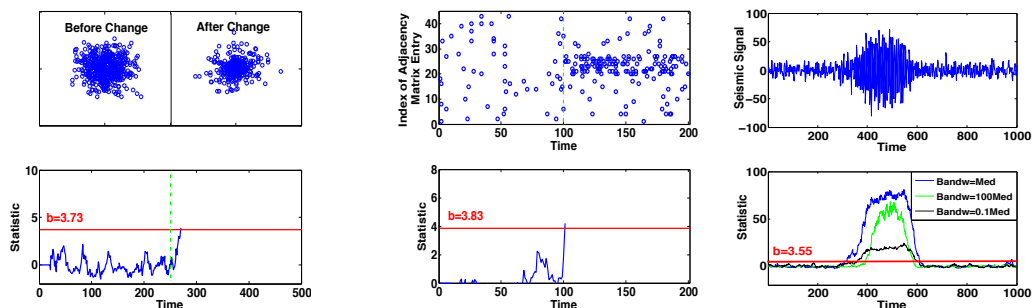
Figure 2: Accuracy of Lemma 1 in estimating the variance of Z_B when $B = 2$ and $B = 200$. Figures show the percentage difference between the estimate from Lemma 1 relative to that obtained from direct Monte Carlo. We form 10000 instances of Z_B using data sampled from the null distribution $\mathcal{N}(0, I_{20})$. Here, “Amount of reference data” denotes the size of pool to sample the six-tuple $(x, x', x'', x''', y, y'')$ to evaluate the quantity in (7).

3.4 Examples of detection statistics

Below, we present a few examples to demonstrate the versatility of scan B -statistics.

Gaussian to Gaussian mixture. In Fig. 3(a), $P = \mathcal{N}(0, I_2)$, Q is a mixture Gaussians: $0.3\mathcal{N}(0, I_2) + 0.7\mathcal{N}(0, 0.1I_2)$, and $\tau = 250$. The online procedure stops at time 270, meaning the change is detected with a small delay of 20 unit time.

Sequence of graphs. In Fig. 3(b), we consider detecting the emergence of a community inside the network modeled using a stochastic block model, which has been considered in (Maragoni-Simonsen and Xie, 2015). Assume that before the change, each sample is a realization of an Erdős-Rényi random graph, with the probability of forming an edge $p_0 = 0.1$ uniform across the graph. After the change, a “community” emerges, which is a subset of nodes, where the edges are formed in between these nodes with much higher probability $p_1 = 0.3$. This models a community where the members inside the community interact more often. Our online procedure stops at time 102, meaning the change is detected with a small delay of 2 unit times.



(a): Gaussian to GMM, $\tau = 250$ (b) Graphs, $\tau = 100$ (c): Real seismic signal

Figure 3: Examples of offline and online B -statistics with $N = 5$. All thresholds (red lines) are theoretical values obtained from Theorem 2 (offline) and Theorem 9 (online).

Real seismic signal; effect of kernel bandwidth. In Fig. 3(c), we consider a segment of real seismic signal that contains a change-point. Using the seismic signal, we also illustrate the effect of kernel bandwidth. The performance of the B -statistic depends on the kernel bandwidth. For Gaussian RBF kernel $k(Y, Y') = \exp(-\|Y - Y'\|^2/2\sigma^2)$, the kernel bandwidth $\sigma > 0$ is typically chosen using a “median trick” (Schölkopf and Smola, 2001), where σ is set to be the median of the pairwise distances between data points. The accuracy of the median trick is justified by Ramdas et al. (2015). The offline B -statistic can detect the seismic event reliably across different choices of the kernel bandwidth.

4. Theoretical approximation of significance level for offline B -statistic

In the offline setting, the choice of the threshold b involves a tradeoff between two standard performance metrics: (1) significance level (SL), which is the probability that the B -statistic exceeds the threshold b under the null hypothesis (i.e., when there is no change); and (2) power, which is the probability of the statistic exceeds the threshold under the alternative hypothesis.

We present an accurate approximation to the SL of the offline B -statistic, assuming the detection threshold b tends to infinity and the number of blocks N is fixed. The following theorem is our main result.

Theorem 2 (SL of offline B -statistic) *When $b \rightarrow \infty$, and $B_{\max} \rightarrow \infty$, with $b/(B_{\max})^{1/2}$ held a fixed positive constant, the significance level of the offline B -statistic defined in (4) is given by*

$$\mathbb{P} \left\{ \max_{2 \leq B \leq B_{\max}} Z'_B > b \right\} = be^{-\frac{1}{2}b^2} \cdot \sum_{B=2}^{B_{\max}} \frac{(2B-1)}{2\sqrt{2\pi}B(B-1)} \nu \left(b\sqrt{\frac{2B-1}{B(B-1)}} \right) \cdot [1 + o(1)], \quad (8)$$

where the special function

$$\nu(\mu) \approx \frac{(2/\mu)(\Phi(\mu/2) - 0.5)}{(\mu/2)\Phi(\mu/2) + \phi(\mu/2)}, \quad (9)$$

$\phi(x)$ and $\Phi(x)$ are the probability density function and the cumulative distribution function of the standard normal distribution, respectively.

We can show numerically that the approximation (8) is accurate even in the non-asymptotic regime. Hence, it is quite useful in choosing a threshold b given a target SL, without having to resort to the onerous numerical simulations. First, consider synthetic data that are *i.i.d.* normal $P = \mathcal{N}(0, I_{20})$. We set B_{\max} to be 50, 100, 150, and in each case, $N = 5$. We compare the thresholds obtained by the theoretical approximation and by simulation, for a prescribed SL α . To obtain threshold by simulation, we generate Monte Carlo trials to for offline B -statistics and find the $(1 - \alpha)$ -quantile as the estimated threshold. Table 1 shows that for various choices of B_{\max} , the thresholds predicted by Theorem 2 match quite well with those obtained by simulation. The accuracy can be further improved for smaller α values, by skewness correction in Section 7.

Next, we consider real speech data from the CENSREC-1-C dataset (more details in Section 8). Here, the null distribution P corresponds to the unknown distribution of the

background signal, and we are interested in detecting the onset of speech signals. This case is more challenging because the true distribution can be arbitrary. In the dataset, there are 3000 reference samples. We bootstrap these reference samples to generate 10000 re-samples to estimate the tail of the detection statistic. Table 2 demonstrates that the thresholds predicted by theory are quite accurate. Note that in this case, the accuracy improves significantly by skewness correction.

Table 1: Thresholds for the offline B -statistics using **synthetic data**, obtained by simulation, theory (Theorem 2), and theory with Skewness Correction (Section 7), respectively, for various SL values α .

α	$B_{\max} = 50$			$B_{\max} = 100$			$B_{\max} = 150$		
	b (sim)	b (theory)	b (SC)	b (sim)	b (theory)	b (SC)	b (sim)	b (theory)	b (SC)
0.10	2.41	2.38	2.57	2.43	2.50	2.76	2.53	2.56	2.89
0.05	2.77	2.67	2.97	2.76	2.78	3.17	2.97	2.83	3.22
0.01	3.54	3.23	3.64	3.47	3.32	3.82	3.64	3.37	3.89

Table 2: Thresholds for the offline B -statistics using **real speech data**, obtained by simulation, theory (Theorem 2), and theory with Skewness Correction (Section 7), respectively, for various SL values α .

α	$B_{\max} = 50$			$B_{\max} = 100$			$B_{\max} = 150$		
	b (boot)	b (theory)	b (SC)	b (boot)	b (theory)	b (SC)	b (boot)	b (theory)	b (SC)
0.10	2.96	2.38	3.23	3.16	2.50	3.59	3.21	2.56	3.94
0.05	3.62	2.67	3.68	3.82	2.78	4.06	3.86	2.83	4.43
0.01	4.85	3.23	4.61	5.20	3.32	5.03	5.42	3.37	5.45

4.1 Proof of main theorem

The key to our approximation is to quantify the tail probability of the detection statistic when the threshold is large. In the offline setting, to quantify the significance level, we are interested in find the probability $\mathbb{P}\{\max_{2 \leq B \leq B_{\max}} Z'_B > b\}$ under the null distribution. The main assumption here is that the collection of random variables $\{Z'_B\}_{B=2, \dots, B_{\max}}$, form a Gaussian random field. This means the finite-dimensional joint distributions of the collection of random variables are all Gaussian, and they are completely specified by its mean and covariance functions, which we characterize below.

Under the null distribution, the expectation $\mathbb{E}[Z'_B]$ is zero since they are constructed using the unbiased MMD estimator. The covariance under the null distribution is given by the following lemma:

Lemma 3 (Covariance structure of Z -statistic in the offline setting) *Under the null distribution, the covariance between two offline B -statistics is given by*

$$r_{u,v} = \text{Cov}(Z'_u, Z'_v) = \sqrt{\binom{u}{2} \binom{v}{2}} / \binom{u \vee v}{2}, \quad 2 \leq u, v \leq B_{\max}, \quad (10)$$

where $u \vee v = \max\{u, v\}$.

The proof can be found in Appendix B.2.

The proof to Theorem 2 is mainly based on the change-of-measure technique. The idea is similar to importance sampling, but it is much more sophisticated. Under null distribution, the boundary exceeding event $\{\max_B Z'_B > b\}$ for a large threshold b is rare (so that false alarm remains low). Since quantify such small probability is hard, we consider an alternative probability measure under which the event happens with much higher probability. Thus, under the new measure, one can use the local central limit theorem to obtain an analytical expression. Finally, the original small probability will be related to the probability under the alternative measure using the Mill's ratio (Yakir, 2013).

Below, we present the main steps of the proof, including (1) exponential tilting; (2) change-of-measure by the likelihood identity; (3) establish properties of the local field and the global term; (4) perform asymptotic approximation using the localization theorem by showing that the “global” log likelihood and the “local process” are asymptotically independent. Finally, we collect terms together to obtain the result.

4.1.1 STEP ONE: EXPONENTIAL TILTING

We first introduce exponential tilting, which creates a family of distributions that is related to the original distribution of B -statistic. Let the log moment generating function of Z'_B be

$$\psi(\theta) = \log \mathbb{E}[e^{\theta Z'_B}]. \quad (11)$$

Define a family of new measures

$$d\mathbb{P}_B = \exp \{ \theta Z'_B - \psi(\theta) \} d\mathbb{P}, \quad (12)$$

where \mathbb{P} represents the original probability measure of Z'_B under the null distribution P , \mathbb{P}_B is the new measure after the transformation, and θ parameterizes the family of new measures. Note that the new measures take the form of exponential family, and θ can be viewed as the natural parameter. It can be verified that \mathbb{P}_B is indeed a probability measure since

$$\int d\mathbb{P}_B = \int \exp \{ \theta Z'_B(x) - \psi(\theta) \} d\mathbb{P} = 1.$$

It can be shown $\dot{\psi}(\theta)$ is equal to the expected value under the tilted measure, since

$$\dot{\psi}(\theta) = \frac{\mathbb{E}[Z'_B e^{\theta Z'_B}]}{\mathbb{E}[e^{\theta Z'_B}]} = \mathbb{E}[Z'_B e^{\theta Z'_B - \psi(\theta)}] = \int x e^{\theta x - \psi(\theta)} d\mathbb{P} = \int x d\mathbb{P}_B.$$

Similarly, one can show that $\ddot{\psi}(\theta)$ equals to the variance under the tilted measure.

Recall that, under the null distribution, Z'_B has zero mean and unit variance, since it is constructed using unbiased MMD estimators and has been divided by the standard deviation. Now we assume Z'_B is a standard Gaussian random variable with zero mean and unit variance. Under this assumption, the corresponding log moment generating function is given by $\psi(\theta) = \theta^2/2$.

One still has the freedom to select the value of θ . We will set the value of θ such that the mean under the tilted measure is equal to a given threshold b . This means that the new measure peaks at the threshold b (this essentially enables us to use the local central limit

theorem later on). This can be done by choosing θ such that $\dot{\psi}(\theta) = b$. Since $\psi(\theta) = \theta^2/2$ for standard normal random variable, this means $\theta = b$. Note that the solution θ does not depend on B . Hence, we can set the mean under the transformed measure to b , by uniformly choosing $\theta = b$ for any B . Given such a choice, the transformed measure is given by $d\mathbb{P}_B = \exp\{bZ'_B(x) - b^2/2\} d\mathbb{P}$. We also define, for each B , the log-likelihood ratio $\log(d\mathbb{P}_B/d\mathbb{P})$ of the form

$$\ell_B = bZ'_B - b^2/2. \quad (13)$$

This way, we have associated the detection statistic Z'_B to a likelihood ratio, even if Z'_B itself does not come out of a likelihood ratio.

The following lemma shows that Z'_B under the new measure has the same unit variance and its mean has been shifted to b . This key fact will lead to the desired exponential tail.

Lemma 4 (Mean and variance under tilted measure) *Define \mathbb{E}_B and Var_B as the expectation and variance under the transformed measures*

$$\mathbb{E}_B[U] = \mathbb{E}[Ue^{\ell_B}], \quad (14)$$

$$\text{Var}_B[U] = \mathbb{E}[U^2e^{\ell_B}] - \mathbb{E}_B^2[U]. \quad (15)$$

We have $\mathbb{E}_B[Z'_B] = b$, and $\text{Var}_B[Z'_B] = 1$.

Proof First, $\mathbb{E}_B[Z'_B] = \dot{\psi}(b) = b$ by construction. To show $\text{Var}_B[Z'_B] = 1$, note that $\log \mathbb{E}[e^{bZ'_B}] = b^2/2$. Taking the derivative of $\psi(\theta)$ with respect to b twice gives $\mathbb{E}[(Z'_B)^2 e^{bZ'_B}] = e^{b^2/2} + b^2 e^{b^2/2}$. Hence, $\mathbb{E}_B[(Z'_B)^2] = \mathbb{E}[(Z'_B)^2 e^{\theta Z'_B - \psi(\theta)}] = 1 + b^2$, and $\text{Var}_B[Z'_B] = \mathbb{E}_B[(Z'_B)^2] - b^2 = 1$. \blacksquare

4.1.2 STEP TWO: CHANGE-OF-MEASURE BY LIKELIHOOD RATIO IDENTITY

Now we are ready to analyze the tail probability. The basic idea is to convert the original problem of finding the small probability that the maximum of a random field exceeds a large threshold, to another problem: finding an alternative measure under which the event happens with a much higher probability.

Here, the alternative measure will be a mixture of simple exponential tilted measures. Define the maximum and the sum for likelihood ratio differences relative to a particular parameter value B :

$$M_B = \max_{s \in \{2, \dots, B_{\max}\}} e^{\ell_s - \ell_B}, \quad S_B = \sum_{s \in \{2, \dots, B_{\max}\}} e^{\ell_s - \ell_B}. \quad (16)$$

Also define a re-centered likelihood ratio, which we call the *global term*

$$\tilde{\ell}_B = b(Z'_B - b).$$

With the definitions above and the log-likelihood ratios ℓ_B in (13), we have the following likelihood ratio identity:

$$\begin{aligned}
 \mathbb{P} \left\{ \max_{2 \leq u \leq B_{\max}} Z'_u > b \right\} &= \mathbb{E} \left[\mathbf{1}; \max_{2 \leq u \leq B_{\max}} Z'_u > b \right] = \mathbb{E} \left[\underbrace{\frac{\sum_{B=2}^{B_{\max}} e^{\ell_B}}{\sum_{s=2}^{B_{\max}} e^{\ell_s}}}_{=1}; \max_{2 \leq u \leq B_{\max}} Z'_u > b \right] \\
 &= \sum_{B=2}^{B_{\max}} \mathbb{E} \left[\frac{e^{\ell_B}}{\sum_s e^{\ell_s}}; \max_{2 \leq u \leq B_{\max}} Z'_u > b \right] \stackrel{(14)}{=} \sum_{B=2}^{B_{\max}} \mathbb{E}_B \left[\frac{1}{\sum_s e^{\ell_s}}; \max_{2 \leq u \leq B_{\max}} Z'_u > b \right] \\
 &= e^{-b^2/2} \sum_{B=2}^{B_{\max}} \mathbb{E}_B \left[\frac{M_B}{S_B} e^{-(\tilde{\ell}_B + \log M_B)}; \tilde{\ell}_B + \log M_B \geq 0 \right]
 \end{aligned} \tag{17}$$

where an intermediate step is done by changing the measure to \mathbb{P}_B , and the last equality can be verified by simple algebra. Recall our notation $\mathbb{E}_B[A; \mathcal{B}] = \mathbb{E}_B[\mathbf{1}\{\mathcal{B}\}A]$ for a random quantity A and event \mathcal{B} ; $\mathbf{1}$ denotes an indicator function.

In a nutshell, the last equation in (17) converts the tail probability to a product of two terms: a deterministic term $e^{-b^2/2}$ associated with the large deviation rate, and a sum of conditional expectations under the transformed measures. A close examination of the conditional expectations of the form $\mathbb{E}_B[\cdots; [\cdots] \geq 0]$ reveals that it involves a product of the ratio M_B/S_B , and an exponential function that depends on $\tilde{\ell}_B$, which plays the role of a weight. Under the new measure \mathbb{P}_B , $\tilde{\ell}_B$ has zero mean and variance equal to b^2 (shown below in Lemma 6) and it dominates the other term $\log M_B$ and, hence, the probability of exceeding zero will happen with much higher probability. Next, we characterize the limiting ratio and the other factors precisely, by the localization theorem.

4.1.3 STEP THREE: ESTABLISH PROPERTIES OF LOCAL FIELD AND GLOBAL TERM

In (17), our target probability has been decomposed into terms that only depend on (i) the *local field* $\{\ell_s - \ell_B\}$, $2 \leq s \leq B_{\max}$, which are the differences between the log-likelihood ratio with parameter B and with other parameter values s , and (ii) the *global term* $\tilde{\ell}_B$, which is the centered and scaled likelihood ratio with parameter B . We need to first establish some useful properties of the local field and global term when using the localization theorem. We will eventually show that the local field and the global term are asymptotically independent.

The following property for the global term can be derived from Lemma 4. The result shows that under the tilted measure, the global term $\tilde{\ell}_B$ is zero mean for any B , with variance diverging with b .

Lemma 5 (Global term for offline B -statistic) *The mean and variance of the global term $\tilde{\ell}_B = b(Z'_B - b)$, for $2 \leq B \leq B_{\max}$, are given by*

$$\mathbb{E}_B[\tilde{\ell}_B] = 0, \quad \text{Var}_B[\tilde{\ell}_B] = b^2, \tag{18}$$

Since we assume Z'_B is approximately normal, the local field $\ell_s - \ell_B$ (or equivalently $b(Z'_s - Z'_B)$) and the global term $\tilde{\ell}_B$ (or equivalently $b(Z'_B - b)$) are also approximately normally distributed.

Lemma 6 (Local field for offline B -statistic) *The mean and variance of the local field $\{\ell_s - \ell_B\}$, for $|s - B| = 0, 1, 2, \dots$, are given by*

$$\mathbb{E}_B[\ell_s - \ell_B] = -b^2(1 - r_{s,B}), \quad \text{Var}_B[\ell_s - \ell_B] = 2b^2(1 - r_{s,B}),$$

with $r_{s,B}$ defined in (10). For any s_1 and s_2 , the covariance between two local field terms is given by

$$\text{Cov}_B(\ell_{s_1} - \ell_B, \ell_{s_2} - \ell_B) = b^2(1 + r_{s_1, s_2} - r_{s_1, B} - r_{s_2, B}).$$

Proof Note that $\ell_s - \ell_B = b(Z'_s - Z'_B)$, $\mathbb{E}_B[Z'_B] = b$, $\text{Var}_B[Z'_B] = 1$. Moreover, due to the normal assumption of Z'_B , we have the following decomposition $\mathbb{E}_B[\ell_s - \ell_B] = \mathbb{E}_B[b(Z'_s - Z'_B)] = \mathbb{E}_B[b(r_{s,B}Z'_B + (1 - r_{s,B})^{1/2}W - Z'_B)] = -b^2(1 - r_{s,B})$, where W is a zero-mean random variable and independent of Z'_B , representing residual of regression. The variance and covariance can be found using similar decompositions. \blacksquare

Remark 7 (Consequence of Lemma 6) *From the expression of the covariance in (10), we have that for $s - B > 0$,*

$$r_{s,B} = [1 + (s - B)/B]^{-1/2} [1 + (s - B)/(B - 1)]^{-1/2},$$

and for $s - B < 0$,

$$r_{s,B} = [1 + (s - B)/B]^{1/2} [1 + (s - B)/(B - 1)]^{1/2}.$$

Consequently,

1. When $|s - B| \rightarrow \infty$, $r_{s,B} \rightarrow 0$. Therefore, when $|s - B| \rightarrow \infty$, $\mathbb{E}_B[\ell_s - \ell_B]$ converges to $-b^2$ and $\text{Var}_B[\ell_s - \ell_B]$ converges $2b^2$.
2. When $|s - B|$ is small, assume $s = B + j$, $j = 0, \pm 1, \pm 2, \dots$. Perform the Taylor expansion of $r_{B+j,B}$ around 0, we have

$$r_{B+j,B} = 1 - \frac{1}{2} \frac{2B - 1}{B(B - 1)} |j| + o(|j|). \quad (19)$$

Define

$$\mu = b\{(2B - 1)/[B(B - 1)]\}^{1/2}. \quad (20)$$

Note that μ depends on the threshold as well as B , the block size parameter. Using (19), we have

$$\begin{aligned} \lim_{|j| \rightarrow 0} \mathbb{E}_B[\ell_{B+j} - \ell_B] &= -\frac{\mu^2}{2} |j|, \\ \lim_{|j| \rightarrow 0} \text{Var}_B[\ell_{B+j} - \ell_B] &= \mu^2 |j|, \\ \lim_{|j_1| \rightarrow 0, |j_2| \rightarrow 0} \text{Cov}_B(\ell_{B+j_1} - \ell_B, \ell_{B+j_2} - \ell_B) &= \mu^2(|j_1| \wedge |j_2|). \end{aligned}$$

Therefore, when $|j|$ is small (i.e., in the neighborhood of zero), we can approximate the local field using a two-sided Gaussian random walk with drift $\mu^2/2$ and variance of the increment being μ^2 :

$$\ell_{B+j} - \ell_B \stackrel{d}{=} \mu \sum_{i=1}^{|j|} \vartheta_i - \mu^2 j/2, \quad j = \pm 1, \pm 2, \dots \quad (21)$$

where ϑ_i are i.i.d. standard normal random variables.

4.1.4 STEP FOUR: APPROXIMATION USING LOCALIZATION THEOREM

The remaining work is to compute the conditional expectations $\mathbb{E}_B[\dots; (\dots) \geq 0]$ for each B in (17). In the following, we drop the subscript B in \mathbb{E}_B for simplicity. We assume $b \rightarrow \infty$, $B_{\max} \rightarrow \infty$, and b^2/B_{\max} is held to a fixed positive constant. Introduce an abstract index κ and let $\kappa = b^2$; this choice is because $\kappa^{1/2}$ is the multiplicative factor that balances the rate of convergence of the global term under the transformed measure. Typically, κ is equal to the variance of the global term, which is equal to b^2 here.

Using a powerful localization theorem (see Theorem 3.1 in (Siegmund et al., 2010) or Theorem 5.2 in (Yakir, 2013)), we can obtain the limit for each term in the summand of (17), rewritten as (by changing the index to κ)

$$\mathbb{E} \left[\frac{M_\kappa}{S_\kappa} e^{-(\tilde{\ell}_\kappa + \log M_\kappa)}; \tilde{\ell}_\kappa + \log M_\kappa \geq 0 \right], \quad (22)$$

when $\kappa \rightarrow \infty$. Basically, the localization theorem states that (22) scaled by $\kappa^{\frac{1}{2}}$ converges to a limit under mild conditions when $\kappa \rightarrow \infty$.

The statement of the theorem involves a local σ -algebra denoted as $\widehat{\mathcal{F}}_\kappa$:

$$\widehat{\mathcal{F}}_\kappa = \sigma\{\ell_s - \ell_B : |s - B| \leq g(\kappa)\}, \quad (23)$$

where a function $g(\kappa)$ specifies the size of the local region. The choice of $g(\kappa)$ is critical and it guarantees subsequent convergence. Following the analysis for scan statistics in (Yakir, 2013), we choose $g(\kappa) = cb^{-2}$ for some large constant c . This local σ -field is asymptotically independent of $\tilde{\ell}_\kappa$, and it carries all information needed to construct the local field.

Define \widehat{M}_κ and \widehat{S}_κ as the maximization and summation restricted to a smaller subset of parameter values $\{s : |s - B| \leq g(\kappa)\}$, and they are measurable with respect to $\widehat{\mathcal{F}}_\kappa$. Note that \widehat{M}_κ and \widehat{S}_κ serve as approximations to M_κ and S_κ . In the limit, the local random field converges to a Gaussian random field, and the ratio $\mathbb{E}[\widehat{M}_\kappa/\widehat{S}_\kappa]$ converges to a limit that can be determined with the parameters of the Gaussian random field.

The localization theorem (Theorem 5.1 in Siegmund et al. (2010) and Sec. 3.4 in Yakir (2013)) consists of five conditions as follows.

Theorem 8 (Localization theorem) *Given $\epsilon > 0$, if for all large κ , all following conditions hold*

- I. Both $0 < M_\kappa \leq S_\kappa < \infty$ and $0 < \widehat{M}_\kappa \leq \widehat{S}_\kappa < \infty$ hold in probability one.

II. Denote $A^c = \{|\log M_\kappa - \log \widehat{M}_\kappa| > \epsilon\} \cup \{|\widehat{S}_\kappa/S_\kappa - 1| > \epsilon\}$. For some $0 < \delta$ that does not depend on ϵ :

$$\max_{|x| \leq 3g(\kappa)} \mathbb{P} \left[A^c \cap \{\tilde{\ell}_\kappa + \log \widehat{M}_\kappa \in x + (0, \delta]\} \cap \{|\hat{m}| \leq g(\kappa)\} \right] \leq \epsilon \kappa^{-1/2},$$

where $\hat{m}_\kappa = \min\{\log \widehat{M}_\kappa, g(\kappa)\} - \log(1 - \epsilon)$.

III. $\mathbb{E}[\widehat{M}_\kappa/\widehat{S}_\kappa]$ converges to a finite and positive limit denoted by $\mathbb{E}[M/S]$.

IV. There exist $\mu_\kappa \in \mathbb{R}$ and $\sigma_\kappa \in \mathbb{R}^+$ such that for every $0 < \epsilon', \delta$, for any event $E \in \widehat{\mathcal{F}}_\kappa$ and for all large enough κ

$$\sup_{|x| \leq \epsilon \kappa^{1/2}} \left| \kappa^{1/2} \mathbb{P}(\tilde{\ell}_\kappa \in x + (0, \delta], E) - \frac{\delta}{\sigma} \phi\left(\frac{\mu}{\sigma}\right) \mathbb{P}(E) \right| \leq \epsilon'.$$

V. $\mathbb{P}(|\log M_\kappa| > \epsilon \kappa^{1/2})$, $\mathbb{P}(|\log \widehat{M}_\kappa| > \epsilon \kappa^{1/2})$ and $\mathbb{P}(\log M_\kappa - \log \widehat{M}_\kappa < -\epsilon)$ are all $o(\kappa^{-1/2})$.

Then

$$\lim_{\kappa \rightarrow \infty} \kappa^{1/2} \mathbb{E} \left[\frac{M_\kappa}{S_\kappa} e^{-[\tilde{\ell}_\kappa + \log M_\kappa]}; \tilde{\ell}_\kappa + \log M_\kappa \geq 0 \right] = \sigma^{-1} \phi\left(\frac{\mu}{\sigma}\right) \mathbb{E}[M/S], \quad (24)$$

where $\phi(\cdot)$ is the density of the standard normal distribution.

Intuitively, the localization theorem says the following. To find the desired limit of (22) as $\kappa \rightarrow \infty$, one first approximates M_κ and S_κ by their localized versions, which are obtained by restricting the maximization and summation in a neighborhood of parameter values. Then one can show that the localized ratio M_κ/S_κ is asymptotic independent of the global term $\tilde{\ell}_\kappa$ as $\kappa \rightarrow \infty$. The asymptotic analysis is then done on the local field and the global term separately. The expected value of the localized ratio $\mathbb{E}[M_\kappa/S_\kappa]$ converges to a constant independent of κ , and the limiting conditional distribution of $\tilde{\ell}_\kappa$ can be found using the local central limit theorem. Thus, one can calculate the remaining conditional expectation involving $\tilde{\ell}_\kappa$.

4.1.5 STEP LAST: CHECKING CONDITIONS

Let us now verify the validity of the conditions in our setting. First, *Condition I* is met since for Gaussian random variables, $M_\kappa > 0$, $S_\kappa > 0$ with probability 1, and the maximization of a collection of non-negative numbers is smaller or equal to the summation. Similar arguments hold for their counterparts $\widehat{M}_\kappa > 0$ and $\widehat{S}_\kappa > 0$ when the maximization and summation are over a smaller set.

Condition II describes that the localized versions \widehat{M}_κ and \widehat{S}_κ are good approximations of M_κ and S_κ when κ is sufficiently large, for properly defined $\widehat{\mathcal{F}}_\kappa$. In Section 3.4.4 of Yakir (2013), the corresponding Condition II has been rigorously checked, assuming a local region defined in the same form of our local region and assuming Gaussian random field. Thus, checking Condition II for our case will follow the same steps, using the properties established in Section 4.1.3. We omit the details here.

Condition III is checked by applying distributional approximations to the localized version of M_κ/S_κ . We can show that the expectation of the ratio $\mathbb{E}[\hat{M}_\kappa/\hat{S}_\kappa]$ converges to a finite and positive limit denoted by $\mathbb{E}[M/S]$, which does not depend on κ . Since the increment $\ell_{B+j} - \ell_B$ has negative mean as shown in Lemma 6, the values of M_κ and S_κ will be determined by values j close to 0, so is the ratio M_κ/S_κ . This implies, a relatively small local region centered on B will be sufficient. From Remark 7, the local field when the index is close to the shifted measure parameter B can be approximated as a two-sided Gaussian random walk with drift $-\mu^2/2$ and variance μ^2 (with μ defined in (20)), which is denoted as $W(\mu^2 j)$ below. Therefore, we have that with high probability,

$$\mathbb{E}[\hat{M}_\kappa/\hat{S}_\kappa] = \mathbb{E} \left[\frac{\max_{|j| \leq cb-2} e^{W(\mu^2 j)}}{\sum_{|j| \leq cb-2} e^{W(\mu^2 j)}} \right]$$

When $c \rightarrow \infty$, it approaches to a limit known as the *Mill's ratio*:

$$\mathbb{E}[M/S] = \mathbb{E} \left[\frac{\max_{|j|} e^{W(\mu^2 j)}}{\sum_{|j|} e^{W(\mu^2 j)}} \right],$$

with maximization and summation extending to the entire collection of negative and positive integers. The Mill's ratio is related to the Laplace transform of the overshoot of the maxima of Gaussian random field over a threshold b , and an expression has been obtained based on nonlinear renewal theory (see, (Siegmund, 1985) and Chapter 2.2 of the book (Yakir, 2013)): $\mathbb{E}[M/S] = \exp(-2 \sum_{j=1}^{\infty} \Phi(-j^{1/2} \mu/2))$. An easier numerical evaluation is given by $\mathbb{E}[M/S] \approx (\mu^2/2)v(\mu)$ for a special function $v(\mu)$ defined in (9).

Condition IV can be checked via a local multivariate central limit theorem that is local in one component and non-local in others (Theorem 5.3 in Yakir (2013)). The theorem says the following: assuming ξ_i are independent, identically distributed random vector of dimension $d+1$. Assume the mean of each vector is zero, and variance of the first component converges to a finite σ , the covariance matrix of the last d components converges a finite matrix Σ , and the correlation between these components and the first one converges to zero (hence, the overall covariance matrix is block-diagonal). Define $S_\gamma = \sum_{i=1}^{\gamma} \xi_{i,1}$ and a d dimensional vector with element $h_{\gamma,j} = \gamma^{-1/2} \xi_{i,j}$, for $1 \leq j \leq d$. Then under mild conditions,

$$\lim_{\gamma \rightarrow \infty} \gamma^{1/2} \mathbb{P}(S_\gamma \in [l, u], h_\gamma \in \mathcal{A}) = \frac{l - u}{(2\pi)^{1/2} \sigma} \mathbb{P}(h \in \mathcal{A}) \quad (25)$$

for any interval $[l, u]$ and an arbitrary set \mathcal{A} .

Our setting matches exactly to the above distribution when we set the global term as the first component and local field as the remaining components. Using the properties in Section 4.1.3, we have shown the finite mean and variance (covariance) of the global and local field terms. We only need to show the global term and the local fields are independent of each other asymptotically. It suffices to prove that the conditional covariance of $\{\ell_{B+j} - \ell_B\}$ given ℓ_B converges to the unconditional covariance, and the conditional means converges to the unconditional one. With a slight abuse of notation, $r_1 = r_{B+j_1, B}$ and $r_2 = r_{B+j_2, B}$. Using the linear regression decomposition, when conditioning on Z'_B (which is proportional

to $\tilde{\ell}_B$), the two local field terms are independent of each other:

$$\begin{aligned} & \text{Cov}(b(Z'_{B+j_1} - Z'_B), b(Z'_{B+j_2} - Z'_B) | Z'_B) \\ &= \text{Cov}(b(r_1 Z'_B + (1 - r_1^2)^{1/2} W_1 - Z'_B), b(r_2 Z'_B + (1 - r_2^2)^{1/2} W_2 - Z'_B) | Z'_B) = 0. \end{aligned}$$

where W_1 and W_2 are two mutually independent zero-mean random variables that represent the regression residuals (they are also independent of Z'_B). On the other hand, using the same decomposition, we can show that without conditioning, the covariance is given by

$$\text{Cov}(b(Z'_{B+j_1} - Z'_B), b(Z'_{B+j_2} - Z'_B)) = b^2(1 - r_1)(1 - r_2).$$

Hence, when $b \rightarrow \infty$, due to the property of local field in equation (19), for $|j_1| \leq cb^{-2}$, $|j_2| \leq cb^{-2}$, the unconditioned covariance converges to zero, which is equal to the conditioned covariance. Similarly, we can show that the conditional means of $\{Z'_{B+j} - Z'_B\}$ conditioning on Z'_B converges to the unconditional ones.

Now we invoke the local central limit theorem. Since the density of the global term $\tilde{\ell}_B$ is approximately normal, we can calculate a desired form of the probability. From (18), the variance of the global term increases with b . The density of $\tilde{\ell}_B$ can be uniformly approximated by $1/(2\pi b^2)^{1/2}$ within a small region around the origin $|x| \leq 3(4 + 1 + \epsilon) \log b$ (Yakir, 2013). Such an approximation also holds for $\tilde{\ell}_B - x$ given any value x that is not too large. Furthermore, notice that $\log \hat{M}_\kappa$ is very close to 0 and therefore is negligible; this is because $e^{\ell_s - \ell_B}$ should attain its maximal value when $|s - B|$ close to 0 as analyzed before. Let $\mu_\kappa = \mathbb{E}_B[\tilde{\ell}_\kappa/b] = 0$ and $\sigma_\kappa^2 = \text{Var}_B[\tilde{\ell}_\kappa/b] = 1$. When $\kappa = b^2 \rightarrow \infty$, using local central limit theorem (25), we have that

$$\kappa^{1/2} \mathbb{P}\left(\tilde{\ell}_\kappa \in x - \log \hat{M}_\kappa + (0, \delta]\right) \rightarrow \frac{\delta}{\sigma_\kappa} \phi\left(\frac{\mu_\kappa}{\sigma_\kappa}\right). \quad (26)$$

Condition V is checked as follows. Note that the terms inside the maximization are likelihood ratios with unit expectation since $\mathbb{E}_B[\exp(\ell_s - \ell_B)] = 1$. This is because from Lemma 6, under the transformed measure, $\ell_s - \ell_B$ is normal random variable with mean $-b^2(1 - r_{s,B})$ and variance $2b^2(1 - r_{s,B})$. Hence, its moment generating function $\mathbb{E}_B[\exp(\theta(\ell_s - \ell_B))] = 1$ for any θ . Thus, $\exp(\ell_s - \ell_B)$ is a martingale and by a standard martingale inequality, $\mathbb{P}(\log M_\kappa > \epsilon \kappa^{1/2}) \leq \exp(-\epsilon \kappa^{1/2})$. Then using a similar argument as in Siegmund et al. (2010), one can show the other two inequalities, since \widehat{M}_κ is an approximation to M_κ .

Finally, since all conditions are met, we can now apply the localization theorem for $b \rightarrow \infty$ and put things together to obtain

$$\mathbb{E}_B \left[\frac{M_B}{S_B} e^{-[\tilde{\ell}_B + \log M_B]}; \tilde{\ell}_B + \log M_B \geq 0 \right] = \frac{\mu^2}{2} \nu(\mu) \frac{1}{\sqrt{2\pi b^2}} (1 + o(1)). \quad (27)$$

Substitute (27) back to the likelihood ratio identity (17), we arrive at the approximation in Theorem 2.

5. Theoretical approximation of ARL for online B -statistic

In the online setting, two commonly used performance metrics are (see, e.g., Xie and Siegmund (2013)): (1) the average run length (ARL), which is the expected time before incorrectly announcing a change of distribution when none has occurred; (2) the expected

detection delay (EDD), which is the expected time to fire an alarm when a change occurs immediately at $\tau = 0$. The EDD considers the worst case and provides an upper bound on the expected delay to detect a change-point when the change occurs later in the sequence of observations.

We present an accurate approximation to the ARL of online B -statistics. The approximation is quite useful in setting the threshold. As a result, given a target ARL, one can determine the corresponding threshold value b from the analytical approximation, avoiding the more expensive numerical simulations. Our main result is the following

Theorem 9 (ARL in online B -statistic) *Let $B_0 \geq 2$. When $b \rightarrow \infty$, the average run length (ARL) of the stopping time T defined in (6) is given by*

$$\mathbb{E}[T] = \frac{e^{b^2/2}}{b} \cdot \left\{ \frac{(2B_0 - 1)}{\sqrt{2\pi}B_0(B_0 - 1)} \cdot \nu \left(b \sqrt{\frac{2(2B_0 - 1)}{B_0(B_0 - 1)}} \right) \right\}^{-1} \cdot [1 + o(1)]. \quad (28)$$

We verify the accuracy of the approximation numerically, by comparing the thresholds obtained by Theorem 9 with those obtained from Monte Carlo simulation. Consider several cases of null distributions: the standard normal $\mathcal{N}(0, 1)$, exponential distribution with mean 1, a Erdős-Rényi random graph with 10 nodes and probability of 0.2 of forming random edges, as well as Laplace distribution with zero mean and unit variance. The simulation results are obtained from 5000 direct Monte Carlo trials. As shown in Fig. 4, the thresholds predicted by Theorem 9 are quite accurate. Fig. 4 also demonstrated that theory is quite accurate for various block sizes (especially for larger B_0). However, we also note that theory tends to underestimate the thresholds. This is especially pronounced for small B_0 , *e.g.*, $B_0 = 50$. The accuracy of the theoretical results can be improved by skewness correction, shown by black lines in Fig. 4, which are discussed later in Section 7.

Theorem 9 shows that ARL is $\mathcal{O}(e^{b^2})$ and, hence, b is $\mathcal{O}((\log \text{ARL})^{1/2})$. Note that EDD is typically on the order of b/Δ due to Wald's identity (Siegmund, 1985), where Δ is the Kullback-Leibler (KL) divergence between the null and alternative distributions (a constant). Hence, given a desired ARL (typically on the order of 5000 or 10000), the error in the estimated threshold will only be translated linearly to EDD. This is a blessing, since it means typically a reasonably accurate b will cause little performance loss in EDD. Similarly, Theorem 2 shows that SL is $\mathcal{O}(e^{-b^2})$ and a similar argument can be made for the offline case.

5.1 Proof sketch of Theorem 9

The method for approximating the ARL is related to what we used to analyze the tail probability of the offline B -statistic. First, we need to establish the following lemma.

Lemma 10 (Asymptotic null distribution of T) *Under the null, when $b \rightarrow \infty$, the stopping time T defined in (6) is uniformly integrable and asymptotically exponentially distributed, *i.e.*,*

$$|\mathbb{P}\{T \geq m\} - \exp(-\lambda_0 m)| \rightarrow 0,$$

in the range where $m\lambda_0$ is bounded away from 0.

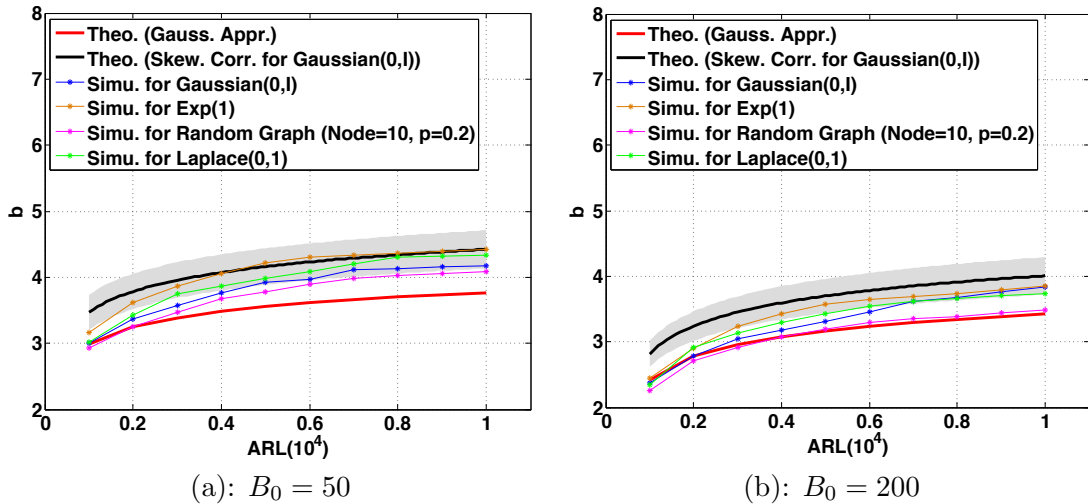


Figure 4: For a range of target ARL values, comparison of thresholds determined from simulation, from Theorem 9, and from theory with the skewness correction (Section 7) under various null distributions. Shaded areas represent standard deviations for skewness-corrected thresholds.

The proof is provided in Appendix C. It is adapted from arguments in Siegmund and Venkatraman (1995); Siegmund and Yakir (2008); Yakir (2009). The main idea is to show that a random variable defined as the number of boundary cross events for detection statistic over disjoint intervals, converges to Poisson random variable in the total variation norm. This is resulted from the Poisson limit theorem (Theorem 1 in Arratia et al. (1989)) for dependent samples.

Using Lemma 10, we know for large m , $\mathbb{P}\{T \geq m\}$ is approximately $1 - \exp(-\lambda_0 m) \approx m\lambda_0$, and $\mathbb{E}\{T\}$ is equal to λ_0^{-1} asymptotically when $b \rightarrow \infty$. So the remaining question is to find the probability and the corresponding λ_0 . Consider $\mathbb{P}\{T \leq m\} = \mathbb{P}\{\max_{2 \leq t \leq m} Z'_{B_0,t} > b\}$. Suppose $m > B_0$ and $\log b \ll m \ll b^{-1}e^{\frac{1}{2}b^2}$. We will adopt a similar strategy to approximate this probability using the change-of-measure technique. Note that the covariance structure for online and offline B -statistic are different, so there will be different drift parameters when we invoke the localization theorem. Using exponential tilting, we introduce a likelihood ratio

$$\zeta_t = bZ'_{B_0,t} - b^2/2.$$

Again using the likelihood ratio identity decomposition, we obtain

$$\mathbb{P}\left\{\max_{2 \leq t \leq m} Z'_{B_0,t} > b\right\} = e^{-b^2/2} \sum_{t=2}^m \mathbb{E}_t \left[\frac{M'_t}{S'_t} e^{-[\tilde{\zeta}_t + \log M'_t]}; \tilde{\zeta}_t + \log M'_t \geq 0 \right], \quad (29)$$

where

$$M'_t = \max_{2 \leq s \leq m} e^{\zeta_s - \zeta_t}, \quad S'_t = \sum_{2 \leq s \leq m} e^{\zeta_s - \zeta_t}, \quad \text{and} \quad \tilde{\zeta}_t = b(Z'_{B_0,t} - b).$$

Hence, one can again apply the localization theorem to find the approximation when $b \rightarrow \infty$, and the only differences are in the definition of global and local field terms.

Lemma 11 (Local field of online B -statistic) *The mean, variance, and covariance of the local field $\{\zeta_s - \zeta_t\}$ are given by*

$$\begin{aligned}\mathbb{E}_t[\zeta_s - \zeta_t] &= -b^2(1 - r_{s,t}), & \text{Var}_t[\zeta_s - \zeta_t] &= 2b^2(1 - r_{s,t}), \\ \text{Cov}_t(\zeta_{s_1} - \zeta_t, \zeta_{s_2} - \zeta_t) &= b^2(1 + r_{s_1, s_2} - r_{s_1, t} - r_{s_2, t}),\end{aligned}$$

where

$$\rho_{s,t} = \text{Cov}(Z'_{B_0, s}, Z'_{B_0, t}) = \frac{\binom{(B_0 - |t-s|) \vee 0}{2}}{\binom{B_0}{2}}. \quad (30)$$

The proof can be found in Appendix B.3. Note that when $|t - s|$ is close to 0, $\mathbb{E}_t[\zeta_s - \zeta_t]$ is close to 0. With an increasing $|t - s|$, $\mathbb{E}_t[\zeta_s - \zeta_t]$ decreases until $|t - s| > B_0$ (when there are no overlapping test data in the sliding block), then $\mathbb{E}_t[\zeta_s - \zeta_t]$ becomes $-b^2$. The values of M_κ and S_κ will be determined by the values of $|j|$ close to 0.

Now, again, we will use an argument based on Taylor expansion to find the drift term of the local field. When $|s - t|$ is close to 0, we can approximate $\{\zeta_s - \zeta_t\}$ as a two-sided random walk. Using Taylor expansion we have

$$\rho_{t+j, t} = 1 - \frac{2B_0 - 1}{B_0(B_0 - 1)}|j| + o(|j|). \quad (31)$$

Let $\lambda = b[2(2B_0 - 1)]/[B_0(B_0 - 1)]^{1/2}$. Hence, we can show that the mean, variance, and covariance of the local field are approximately

$$\begin{aligned}\lim_{|j| \rightarrow 0} \mathbb{E}_t[\zeta_{t+j} - \zeta_t] &= -\frac{\lambda^2}{2}|j|, \\ \lim_{|j| \rightarrow 0} \text{Var}_t[\zeta_{t+j} - \zeta_t] &= \lambda^2|j|, \\ \lim_{|j_1| \rightarrow 0, |j_2| \rightarrow 0} \text{Cov}_t(\zeta_{t+j_1} - \zeta_t, \zeta_{t+j_2} - \zeta_t) &= \lambda^2(|j_1| \wedge |j_2|).\end{aligned}$$

As a result, by invoking the localization theorem through a similar set of steps, we obtain

$$\mathbb{P}\{T \leq m\} = m \cdot \frac{be^{-\frac{1}{2}b^2}}{\sqrt{2\pi}} \frac{(2B_0 - 1)}{B_0(B_0 - 1)} \cdot \nu \left(b \sqrt{\frac{2(2B_0 - 1)}{B_0(B_0 - 1)}} \right) (1 + o(1)), \quad (32)$$

Matching this to above, we know λ_0 is the factor that multiplies m and this leads to the desired result.

6. Study of power and expected detection delay

In this section, we study the detection power and the expected detection delay of the offline and online B -statistics, respectively, by comparing with classic methods.

6.1 Offline change-point detection: Comparison with parametric statistics

We compare the offline B -statistic with two commonly used parametric test statistics: the Hotelling's T^2 and the generalized likelihood ratio (GLR) statistics. Assume samples $\{x_1, x_2, \dots, x_n\}$.

Hotelling's T^2 statistic. For a hypothetical change-point location k , the statistic measures the quadratic distance of the sample means in two segments $[1, k]$ and $[k + 1, t]$ in the quadratic distance defined by the sample covariance matrix:

$$T^2(k) = \frac{k(n-k)}{n} (\bar{x}_k - \bar{x}_k^*)^T \widehat{\Sigma}^{-1} (\bar{x}_k - \bar{x}_k^*),$$

where, $\bar{x}_k = \sum_{i=1}^k x_i/k$, $\bar{x}_k^* = \sum_{i=k+1}^n x_i/(n-k)$ and the pooled covariance estimator

$$\widehat{\Sigma} = (n-2)^{-1} \left(\sum_{i=1}^k (x_i - \bar{x}_i)(x_i - \bar{x}_i)^T + \sum_{i=k+1}^n (x_i - \bar{x}_i^*)(x_i - \bar{x}_i^*)^T \right).$$

The Hotelling's T^2 test detects a change whenever $\max_{1 \leq k \leq n} T^2(k)$ exceeds a threshold.

The **generalized likelihood ratio (GLR)** statistic can be derived by assuming the null and the alternative distributions are two multivariate normal distributions when both the mean and the covariance matrix change, and the parameters all unknown. For a hypothetical change-point location k , the GLR statistic is given by

$$\ell(k) = n \log |\widehat{\Sigma}_n| - k \log |\widehat{\Sigma}_k| - (n-k) \log |\widehat{\Sigma}_k^*|,$$

where $\widehat{\Sigma}_k = k^{-1} \left(\sum_{i=1}^k (x_i - \bar{x}_i)(x_i - \bar{x}_i)^T \right)$, and $\widehat{\Sigma}_k^* = (n-k)^{-1} \sum_{i=k+1}^n (x_i - \bar{x}_i^*)(x_i - \bar{x}_i^*)^T$. The GLR statistic detects a change whenever $\max_{1 \leq k \leq n} \ell(k)$ exceeds a threshold.

For our examples, we set $n = B_{\max} = 200$ for the Hotelling and the B -statistic, respectively. Let the change-point occurs at $\tau = 100$, and choose the SL $\alpha = 0.05$ (the probability of incorrectly detecting a change under the null). Thresholds for the offline B -statistic are obtained from Theorem 2 and for the other two methods are obtained from simulations. Consider the following cases:

Case 1 (mean shift): observe a sequence of observations in \mathbb{R}^{20} , whose distribution shifts from $\mathcal{N}(\mathbf{0}, I_{20})$ to $\mathcal{N}(0.1\mathbf{e}, I_{20})$;

Case 2 (mean shift with larger magnitude): observe a sequence of observations in \mathbb{R}^{20} , whose distribution shifts from $\mathcal{N}(\mathbf{0}, I_{20})$ to $\mathcal{N}(0.2\mathbf{e}, I_{20})$;

Case 3 (mean and local covariance change): observe a sequence of observations in \mathbb{R}^{20} , whose distribution shifts from $\mathcal{N}(\mathbf{e}, I_{20})$ to $\mathcal{N}(0.2\mathbf{e}, \Sigma)$, where $[\Sigma]_{11} = 2$ and $[\Sigma]_{ii} = 1$, $i = 2, \dots, 20$;

Case 4 (Gaussian to Laplace): observe a sequence of one-dimensional observations, whose distribution shifts from $\mathcal{N}(0, 1)$ to Laplace distribution with zero mean and unit variance. Note that the mean and the variance remain the same after the change.

We estimate the power for each case using 100 Monte Carlo trials. Table 3 shows that the B -statistic achieves higher power than the Hotelling's T^2 statistic and the GLR statistic in all cases. The GLR statistic performs poorly, since when k small or closer to n , it needs to estimate the pre-change and post-change sample covariance matrix using a limited number of samples.

Table 3: Comparison of detection power for offline change-point detection. Thresholds for all methods are calibrated so that the significance level is $\alpha = 0.05$.

	Case 1	Case 2	Case 3	Case 4
B -statistic	0.71	1.00	1.00	0.44
Hotelling's T^2	0.18	0.88	0.87	0.03
GLR	0.03	0.05	0.12	0.04

6.2 Online change-point detection: Comparison with Hotelling's T^2 statistic

Now consider online B -statistic with a fixed block-size $B_0 = 20$. We compare the online B -statistic with a Shewhart chart based on Hotelling's T^2 statistic¹. At each time t , we form a Hotelling's T^2 statistic using the past B_0 samples in $[t - B_0 + 1, t]$,

$$T^2(t) = B_0(\bar{x}_t - \hat{\mu})^T \widehat{\Sigma}_0^{-1}(\bar{x}_t - \hat{\mu}_0),$$

where $\bar{x}_t = (\sum_{i=t-B_0+1}^t x_i)/B_0$, and $\hat{\mu}_0$ and $\widehat{\Sigma}_0$ are estimated from reference data. The procedure detects a change-point whenever $T^2(t)$ exceeds a threshold for the first time. The threshold for online B -statistic is obtained from Theorem 9, and from simulations for the Hotelling's T^2 statistic. To simulate EDD, let the change occur at the first point of the testing data. Consider the following cases:

Case 1 (mean shift): distribution shifts from $\mathcal{N}(\mathbf{0}, I_{20})$ to $\mathcal{N}(0.3\mathbf{1}, I_{20})$;

Case 2 (covariance change): distribution shifts from $\mathcal{N}(\mathbf{0}, I_{20})$ to $\mathcal{N}(\mathbf{0}, \Sigma)$, where $[\Sigma]_{ii} = 2$, where $i = 1, 2, \dots, 5$ and $[\Sigma]_{ii} = 1$, $i = 6, \dots, 20$;

Case 3 (covariance change): distribution shifts from $\mathcal{N}(\mathbf{0}, I_{20})$ to $\mathcal{N}(\mathbf{0}, 2I_{20})$;

Case 4 (Gaussian to Gaussian mixture): distribution shifts from $\mathcal{N}(\mathbf{0}, I_{20})$ to mixture Gaussian $0.3\mathcal{N}(\mathbf{0}, I_{20}) + 0.7\mathcal{N}(\mathbf{0}, 0.1I_{20})$;

Case 5 (Gaussian to Laplace)²: distribution shifts from $\mathcal{N}(0, 1)$ to Laplace distribution with zero mean and unit variance.

We evaluate the EDD for each case using 500 Monte Carlo trials. The results are summarized in Table 4. Note that in detecting changes in either Gaussian mean or covariance, the online B -statistic performs competitively with Hotelling's T^2 , which is tailored to the Gaussian distribution. In the more challenging scenarios such as Case 4 and Case 5, the Hotelling's T^2 completely fails to detect the change-point whereas the online B -statistic can detect the change fairly quickly.

7. Skewness correction

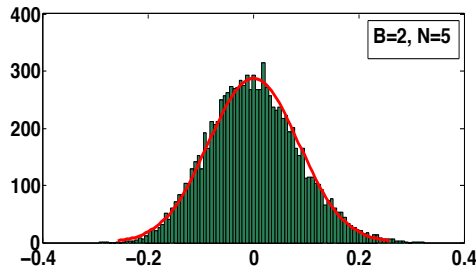
We have shown that approximations to SL and ARL, assuming that Z'_B are normally distributed, are reasonably accurate. However, Z'_B does not converge to normal distribution even when B is large (see Appendix G) and it has a nonvanishing skewness, as illustrated

1. Here we do not compare the online B -statistic with the GLR statistic, since in our experiments Hotelling's T^2 consistently outperforms GLR when dimension is large.
 2. For this difficult case, we report the EDD comparisons based on the selected 500 sequences where B -statistic can successfully detect the changes which are defined as crossing the threshold within 50 steps once the change occurs. Hotelling's T^2 fails to detect the changes for all sequences.

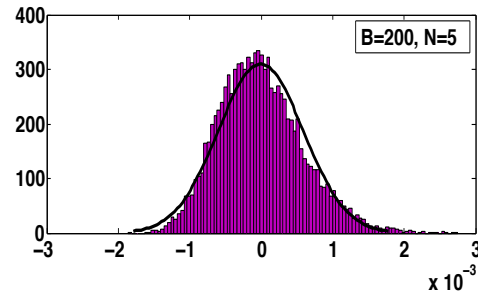
Table 4: Comparison of EDD in online change-point detection. The parameter is $B_0 = 20$ and thresholds for all methods are calibrated so that $ARL = 5000$. Dashed line – means that the procedure fails to detection the change, i.e., EDD is longer than 50.

	Case 1	Case 2	Case 3	Case 4	Case 5
B -statistic	4.20	9.10	1.00	23.38	23.03
Hotelling's T^2	2.47	25.46	1.27	–	–

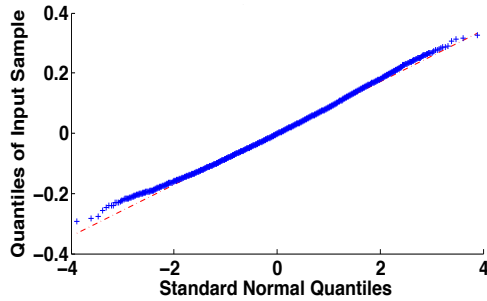
by the following numerical example. Form 10000 instances of Z_B computed using samples from $\mathcal{N}(0, I_{20})$. Figs. 5(a)-(b) show the empirical distributions of Z_B when $N = 5$, and $B = 2$ or $B = 200$, respectively. Also plotted are the Gaussian probability density functions with mean equal to the sample mean, and the variance predicted by Lemma 1. Note that the empirical distributions of Z_B match with Gaussian distributions to a certain extent but the skewness becomes larger for larger B . Figs. 5(c)-(d) show the corresponding Q-Q plots.



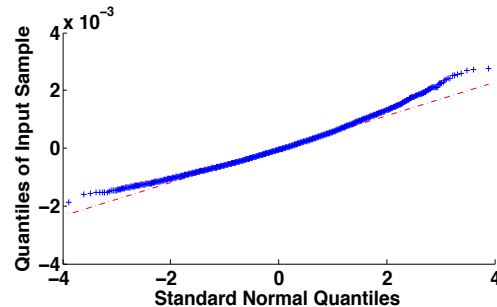
(a): $B = 2, N = 5$, empirical distribution



(b): $B = 200, N = 5$, empirical distribution



(c): $B = 2, N = 5$, Q-Q plot



(d): $B = 200, N = 5$, Q-Q plot

Figure 5: Empirical distributions of Z_B when $B = 2$ and $B = 200$, respectively. Note that although Gaussian distribution seems to be a reasonable fit to the statistic, the skewness becomes larger for larger B .

Incorporating the skewness of Z_B , one can improve the accuracy of the approximations for SL in Theorem 2 and for ARL in Theorem 9. Note that the log-moment-generating function $\psi(\theta)$ defined in (11) corresponds to the so-called cumulant generating function

(McCullagh and Kolassa, 2009) and it has an expansion for θ close to zero:

$$\psi(\theta) = \kappa_1\theta + \frac{\kappa_2}{2}\theta^2 + \frac{\kappa_3}{3!}\theta^3 + o(\theta^3).$$

Since $\mathbb{E}[Z'_B] = 0$, the cumulants take values $\kappa_1 = \mathbb{E}[Z'_B] = 0$, $\kappa_2 = \text{Var}[Z'_B] = 1$, $\kappa_3 = \mathbb{E}[(Z'_B)^3] - 3\mathbb{E}[(Z'_B)^2]\mathbb{E}[Z'_B] + 2(\mathbb{E}[Z'_B])^3 = \mathbb{E}[(Z'_B)^3]$. Recall that when deriving approximations using change-of-measurement, we choose parameter θ such that the moment generating function $\dot{\psi}(\theta) = b$. If Z'_B is a standard normal, $\psi(\theta) = \theta^2/2$, and hence $\theta = b$. Now with skewness correction, we approximate $\psi(\theta)$ as $\theta^2/2 + \kappa_3\theta^3/6$ when solving for θ . Hence, we solve for

$$\dot{\psi}(\theta) \approx \theta + \mathbb{E}[(Z'_B)^3]\theta^2/2 = b,$$

and denote the solution to be θ_B (note that this time the solution may depend on B). Moreover, with skewness correction, we will change the leading exponent term in (8) and (32) from $e^{-b^2/2}$ to be $e^{\psi(\theta'_B) - \theta'_B b}$. From numerical experiments, we find that the skewness correction is especially useful when SL is small (*e.g.*, $\alpha = 0.01$) for the offline case or when block size B_0 is small (see Table 1, 2 and Fig. 4). The skewness correction can be important, since it appears in the exponent of the expressions.

The remaining task is to estimate the skewness of B -statistic. Since Z_B is zero-mean, the skewness of Z'_B is related to the variance and third moment of Z_B via

$$\kappa_3 = \mathbb{E}[(Z'_B)^3] = \text{Var}[Z_B]^{-3/2}\mathbb{E}[Z_B^3].$$

We already know how to estimate the variance of Z_B from Lemma 1. The following lemma express the third-order moment $\mathbb{E}[Z_B^3]$ in terms of the moments of the kernel h defined in (2):

Lemma 12 (Third-order moment of Z_B)

$$\begin{aligned} \mathbb{E}[Z_B^3] = & \frac{8(B-2)}{B^2(B-1)^2} \left\{ \frac{1}{N^2} \mathbb{E} [h(x, x', y, y')h(x', x'', y', y'')h(x'', x, y'', y)] \right. \\ & + \frac{3(N-1)}{N^2} \mathbb{E} [h(x, x', y, y')h(x', x'', y', y'')h(x''', x''', y''', y''')] \\ & \left. + \frac{(N-1)(N-2)}{N^2} \mathbb{E} [h(x, x', y, y')h(x'', x''', y', y'')h(x''', x''', y''', y''')] \right\} \\ & + \frac{4}{B^2(B-1)^2} \left\{ \frac{1}{N^2} \mathbb{E} [h(x, x', y, y')^3] \right. \\ & + \frac{3(N-1)}{N^2} \mathbb{E} [h(x, x', y, y')^2h(x'', x''', y, y')] \\ & \left. + \frac{(N-1)(N-2)}{N^2} \mathbb{E} [h(x, x', y, y')h(x'', x''', y, y')h(x''', x''', y''', y''')] \right\}. \end{aligned} \quad (33)$$

Lemma 12 enables us to estimate the skewness efficiently, by reducing it to evaluating simpler terms in (33) that only requires estimating the statistic of the kernel function $h(\cdot, \cdot, \cdot, \cdot)$ with tuples of samples. For instance, to evaluate $\mathbb{E} [h(x, x', y, y')h(x', x'', y', y'')h(x'', x, y'', y)]$, we may each time draw a tuple of six samples without replacement from the reference data,

treat them as x, x', x'', y, y' and y'' , compute the value of the function, repeat this many times, and take average.

Finally, although Z'_B does not converge to Gaussian, the difference between its moment generating functions and that the standard normal distribution can be bounded, as we show below. By applying a result on Page 220 of Yakir (2013), we have

$$\left| \mathbb{E}[e^{\theta Z'_B}] - \left(1 + \frac{\theta^2}{2}\right) \right| \leq \min\left\{\frac{|\theta|^3}{6} \mathbb{E}[|Z'_B|^3], \theta^2 \mathbb{E}[|Z'_B|^2]\right\}.$$

and if considering the skewness κ_3 of Z'_B , we have

$$\left| \mathbb{E}[e^{\theta Z'_B}] - \left(1 + \frac{\theta^2}{2} + \frac{\theta^3 \kappa_3}{6}\right) \right| \leq \min\left\{\frac{\theta^4}{24} \mathbb{E}[|Z'_B|^4], \frac{1}{3} |\theta|^3 \mathbb{E}[|Z'_B|^3]\right\}.$$

8. Real-data

We test the performance of scanning B -statistics for change-point detection on real data. Our datasets include: (1) CENSREC-1-C: a real-world speech data set in the Speech Resource Consortium (SRC) corpora provided by National Institute of Informatics (NII)³; (2) Human Activity Sensing Consortium (HASC) challenge 2011 data⁴. We compare our modified B -statistic with a baseline algorithm, the relative density-ratio (RDR) estimate (Song et al., 2013). One limitation of the RDR algorithm, however, is that it is not suitable for high-dimensional data because estimating density ratio in the high-dimensional setting is an ill-posed problem. To achieve reasonable performance for the RDR algorithm, we adjust the bandwidth and the regularization parameter at each time step and, hence, the RDR algorithm is computationally more expensive than using B -statistics. We adopt the Area Under Curve (AUC) (Song et al., 2013) as a performance metric: the larger the AUC, the better.

Our modified B -statistics have very competitive performance compared with the baseline RDR algorithm on the real data. Here we only report the main results and leave the details in Appendix E. For speech data, our goal is to detect online the onset of a speech signal emergent from the background. The backgrounds are taken from real acoustic signals, such as noise in highway, airport and subway stations. The overall AUC for the B -statistic is **0.8014** and for the baseline algorithm is **0.7578**. For human activity detection data, our goal is to detect a transition from one activity to another as quickly as possible. Each instance consists six possible of human activity data collected by portable three-axis accelerometers. The overall AUC for the B -statistic is **0.8871** and for the baseline algorithm is **0.7161**.

9. Discussions

There are a few possible directions to extend our scan B -statistics. (1) Thus far, we have assumed that data are *i.i.d.* from a null distribution P and when the change happens, data are *i.i.d.* from an alternative distribution Q . Under these assumptions, we have developed

3. Available from <http://research.nii.ac.jp/src/en/CENSREC-1-C.html>

4. Available from <http://hasc.jp/hc2011>

the offline and online change-point detection algorithms based on the kernel two-sample test statistic MMD. One may relax the temporal independence assumption and extend B -statistics for dependent data by incorporating ideas from (Chwialkowski and Gretton, 2014). (2) We have demonstrated how the number of blocks and block size affect the performance of B -statistics. One can also explore how kernel bandwidth, as well as the dimensionality of the data, would affect the performance. An empirical observation is that the performance of MMD statistic degrades with the increasing dimensions in data. Some recent results for kernel based test can be found in (Ramdas et al., 2015). We may adopt the idea of (Ramdas et al., 2015) to extend our modified B -statistics for detecting a change in the dependence. (3) For an exceedingly high dimensional data set with large Gram matrix, one can perform random subsampling to reduce complexity similar to (Xie et al., 2015).

Acknowledgement

This research was supported in part by NSF CMMI-1538746, NSF CCF-1442635, NSF CAREER CCF-1650913, a grant from Atlanta Police Foundation, gift donation from Adobe Research to Yao Xie; NSF/NIH BIGDATA 1R01GM108341, ONR N00014-15-1-2340, NSF IIS-1218749, NSF IIS-1639792, NSF CAREER IIS-1350983, grant from Intel and NVIDIA to Le Song.

References

- S. Arlot, A. Celisse, and Z. Harchaoui. Kernel change-point detection. *arXiv preprint arXiv:1202.3878*, 6, 2012.
- R. Arratia, L. Goldstein, and L. Gordon. Two moments suffice for Poisson approximations: the Chen-Stein method. *The Annals of Probability*, pages 9–25, 1989.
- M. Bibinger, M. Jirak, M. Vetter, et al. Nonparametric change-point analysis of volatility. *The Annals of Statistics*, 45(4):1542–1578, 2017.
- E. Brodsky and B. Darkhovsky. *Nonparametric methods in change point problems*, volume 243. Springer Science & Business Media, 2013.
- K. Chwialkowski and A. Gretton. A kernel independence test for random processes. In *International Conference on Machine Learning (ICML)*, 2014.
- M. Csörgő and L. Horváth. Invariance principles for changepoint problems. *Journal of Multivariate Analysis*, 27(1):151–168, 1988.
- M. Csörgő and L. Horváth. *Limit theorems in change-point analysis*, volume 18. John Wiley & Sons Inc, 1997.
- H. Dehling, R. Fried, I. Garcia, and M. Wendler. Change-point detection under dependence based on two-sample u -statistics. In *Asymptotic Laws and Methods in Stochastics*, pages 195–220. Springer, 2015.
- A. Dembo and O. Zeitouni. *Large deviations techniques and applications*. Springer, 2nd edition, 2009.

- F. Desobry, M. Davy, and C. Doncarli. An online kernel change detection algorithm. *IEEE Transactions on Signal Processing*, 53(8):2961–2974, 2005.
- F. Enikeeva and Z. Harchaoui. High-dimensional change-point detection with sparse alternatives. *arXiv:1312.1900*, 2014.
- G. Fasano and A. Franceschini. A multidimensional version of the kolmogorov–smirnov test. *Monthly Notices of the Royal Astronomical Society*, 225(1):155–170, 1987.
- L. Gordon and M. Pollak. An efficient sequential nonparametric scheme for detecting a change of distribution. *Annals of Statistics*, 22(2):763–804, 1994.
- A. Gretton, K.M. Borgwardt, M.J. Rasch, B. Schölkopf, and A. Smola. A kernel two-sample test. *The Journal of Machine Learning Research*, 13(1):723–773, 2012.
- Z. Harchaoui and O. Cappé. Retrospective mutiple change-point estimation with kernels. In *IEEE Workshop on Statistical Signal Processing (SSP)*, pages 768–772. IEEE, 2007.
- Z. Harchaoui, F. Bach, and E. Moulines. Kernel change-point analysis. In *Advances in Neural Information Processing Systems (NIPS)*, 2008.
- Z. Harchaoui, F. Bach, O. Cappe, and E. Moulines. Kernel-based methods for hypothesis testing. *IEEE Signal Processing Magazine*, pages 87–97, 2013.
- F. J. Massey Jr. The kolmogorov-smirnov test for goodness of fit. *Journal of the American statistical Association*, 46(253):68–78, 1951.
- D. Kifer, S.B. David, and J. Gehrke. Detecting change in data streams. In *Proceedings of the 30th International Conference on Very Large Data Bases-Volume 30*, pages 180–191. VLDB Endowment, 2004.
- H.W. Lilliefors. On the kolmogorov-smirnov test for normality with mean and variance unknown. *Journal of the American statistical Association*, 62(318):399–402, 1967.
- D. Maragoni-Simonsen and Y. Xie. Sequential changepoint approach for online community detection. *IEEE Signal Processing Letters*, 22(8):1035–1039, 2015.
- D. Matteson and N. James. A nonparametric approach for multiple change point analysis of multivariate data. *Journal of the American Statistical Association*, 109(505):334–345, 2014.
- P. McCullagh and J. Kolassa. Cummulants. *Scholarpedia*, 4(3):4699, 2009.
- D. Picard. Testing and estimating change-points in time series. *Advances in applied probability*, 17(04):841–867, 1985.
- A. Ramdas, S.J. Reddi, B. Póczos, A. Singh, and L. Wasserman. On the decreasing power of kernel and distance based nonparametric hypothesis tests in high dimensions. In *Twenty-Ninth AAAI Conference on Artificial Intelligence (AAAI)*, 2015.

- Z. E. Ross and Y. Ben-Zion. Automatic picking of direct P , S seismic phases and fault zone head waves. *Geophysical Journal International*, 2014.
- B. Schölkopf and A. Smola. *Learning with kernels: support vector machines, regularization, optimization, and beyond*. MIT press, 2001.
- B. Schölkopf and A. Smola. *Learning with kernels*. MIT Press, Cambridge, MA, 2002.
- B. Schölkopf, K. Tsuda, and J.-P. Vert. *Kernel methods in computational biology*. MIT Press, Cambridge, MA, 2004.
- R. Serfling. *Approximation theorems of mathematical statistics*, volume 162. John Wiley & Sons, 2009.
- R. J. Serfling. *U-Statistics*. Approximation theorems of mathematical statistics. John Wiley & Sons, 1980.
- D. Siegmund. *Sequential analysis: tests and confidence intervals*. Springer, 1985.
- D. Siegmund and E. S. Venkatraman. Using the generalized likelihood ratio statistic for sequential detection of a change-point. *Annals of Statistics*, (23):255–271, 1995.
- D. Siegmund and B. Yakir. Detecting the emergence of a signal in a noisy image. *Statistics and Its Inference*, (1):3–12, 2008.
- D. Siegmund, B. Yakir, and N. Zhang. Tail approximations for maxima of random fields by likelihood ratio transformations. *Sequential Analysis*, 29(3):245–262, 2010.
- L. Song, Y. Makoto, C. Nigel, and S. Masashi. Change-point detection in time-series data by direct density-ratio estimation. *Neural Networks*, 43:72–83, 2013.
- A. Tartakovsky, I. Nikiforov, and M. Basseville. *Sequential analysis: Hypothesis testing and changepoint detection*. CRC Press, 2014.
- T. Wan, K. Qu, Q. C. Zhang, R. A. Flynn, O. Manor, Z. Ouyang, J. Zhang, R. C. Spitale, M.P. Snyder, E. Segal, et al. Landscape and variation of rna secondary structure across the human transcriptome. *Nature*, 505(7485):706, 2014.
- T. Wang, J. J. Wei, D.M. Sabatini, and E.S. Lander. Genetic screens in human cells using the crispr-cas9 system. *Science*, 343(6166):80–84, 2014.
- R. Wilcox. Kolmogorov–smirnov test. *Encyclopedia of biostatistics*, 2005.
- B. Xie, Y. Liang, and L. Song. Scale up nonlinear component analysis with doubly stochastic gradients. In *Advances in neural information processing systems (NIPS)*, 2015.
- Y. Xie and D. Siegmund. Sequential multi-sensor change-point detection. *Annals of Statistics*, 41(2):670–692, 2013.
- B. Yakir. Multi-channel change-point detection statistic with applications in dna copy-number variation and sequential monitoring. In *Proceedings of Second International Workshop in Sequential Methodologies*, pages 15–17, 2009.

B. Yakir. *Extremes in random fields: A theory and its applications*. Wiley, 2013.

W. Zaremba, A. Gretton, and M. Blaschko. B -test: low variance kernel two-sample test. In *Advances in Neural Information Processing Systems (NIPS)*, 2013.

C. Zou, G. Yin, L. Feng, Z. Wang, et al. Nonparametric maximum likelihood approach to multiple change-point problems. *The Annals of Statistics*, 42(3):970–1002, 2014a.

S. Zou, Y. Liang, H. V. Poor, and X. Shi. Nonparametric detection of anomalous data via kernel mean embedding. *arXiv:1405.2294*, 2014b.

Appendix A. Recursive implementation of online B -statistic

The online B -statistic can be computed recursively via a simple update scheme. By its construction, when time elapses from t to $(t + 1)$, a new sample is added into the post-change block, and the oldest sample is moved to the reference pool. Each reference block is updated similarly by adding one sample randomly drawn from the pool of reference data, and the oldest sample is purged. Hence, only a limited number of entries in the Gram matrix that are due to the new sample need to be updated. The update scheme is illustrated in Fig. 6 and explained in more details therein. The recursive scheme reduces the computational cost of the online B -statistic to be *linear in time*. Similarly, the offline B -statistic can also be computed recursively by utilizing the fact that Z_B for $B \in \{2, \dots, B_{\max}\}$ shares many common terms. The recursive scheme reduces the computational cost of the offline B -statistic to be $\mathcal{O}(NB_{\max}^2)$.

Appendix B. Variance and covariance calculation

Below, $X_{i,j}^{(B)}$, where $i = 1, \dots, N$, and $j = 2, \dots, B_{\max}$, denotes the j -th sample in the i -th block $X_i^{(B)}$, and $Y_j^{(B)}$ denotes the j -th sample in $Y^{(B)}$. The superscript B denotes the block size. We start with proving Lemma 13 and Lemma 14, which are useful in proving Lemma 1.

Lemma 13 (Variance of MMD, under the null.) *Under the null hypothesis,*

$$\text{Var} \left[\text{MMD}^2(X_i^{(B)}, Y^{(B)}) \right] = \binom{B}{2}^{-1} \mathbb{E}[h^2(x, x', y, y')], \quad i = 1, \dots, N. \quad (34)$$

Proof For notational simplicity, below we drop the superscript B . Furthermore, we use x , x' , y and y' to denote generic samples, i.e., $X_{i,l} \stackrel{d}{=} x$, $X_{i,j} \stackrel{d}{=} x'$, $Y_l \stackrel{d}{=} y$, $Y_j \stackrel{d}{=} y'$ and they are mutually independent of each other. Here the notation $\stackrel{d}{=}$ means two random variables have the same distribution. Below, we follow the same convention. For any $i = 1, 2, \dots, n$,

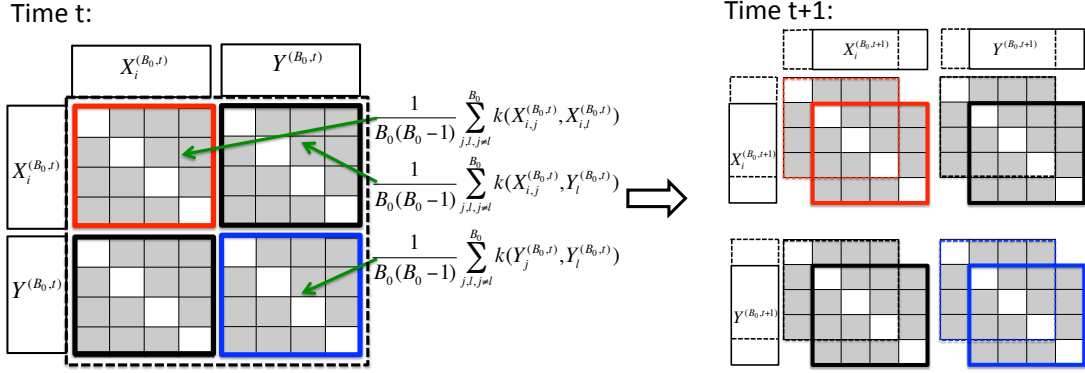


Figure 6: Recursive update scheme to compute the online B -statistics. The online B -statistic is formed with N background blocks and one testing block and, hence, we keep track of N Gram matrices. For illustration purposes, we partition the Gram matrix into four windows (in red, black and blue, as shown on the left panel). At time t , to obtain $\text{MMD}^2(X_i^{(B_0,t)}, Y^{(B_0,t)})$, we compute the shaded elements and take an average within each window. The diagonal entries in each window are removed to obtain an unbiased estimate. At time $t + 1$, we update $X_i^{(B_0,t)}$ and $Y^{(B_0,t)}$ with the new data point and purge the oldest data point, and update the Gram matrix by moving the colored window as shown on the right panel, computing the elements within the new windows, and taking an average. Note that we only need to compute the right-most column and the bottom row.

by definition of U-statistic, we have

$$\begin{aligned}
 \text{Var} [\text{MMD}^2(X_i, Y)] &= \text{Var} \left[\binom{B}{2}^{-1} \sum_{l < j} h(X_{i,l}, X_{i,j}, Y_l, Y_j) \right] \\
 &= \binom{B}{2}^{-2} \left[\binom{B}{2} \binom{2}{1} \binom{B-2}{2-1} \text{Var} [\mathbb{E}_{x,y} [h(x, x', y, y')]] \right. \\
 &\quad \left. + \binom{B}{2} \binom{2}{2} \binom{B-2}{2-2} \text{Var} [h(x, x', y, y')] \right].
 \end{aligned} \tag{35}$$

Under null distribution, $\mathbb{E}_{x,y} [h(x, x', y, y')] = 0$. Thus, $\text{Var} [\mathbb{E}_{x,y} [h(x, x', y, y')]] = 0$, and

$$\text{Var} [h(x, x', y, y')] = \mathbb{E}[h^2(x, x', y, y')] - \mathbb{E}[h(x, x', y, y')]^2 = \mathbb{E}[h^2(x, x', y, y')].$$

Substitute these results into (35), we obtain the desired result (34). ■

Lemma 14 (Covariance of MMD, under the null, same block size.) For $s \neq 0$, under null hypothesis

$$\begin{aligned} & \text{Cov} \left[\text{MMD}^2(X_i^{(B)}, Y^{(B)}), \text{MMD}^2(X_{i+s}^{(B)}, Y^{(B)}) \right] \\ &= \binom{B}{2}^{-1} \text{Cov} [h(x, x', y, y'), h(x'', x''', y, y')]. \end{aligned}$$

Proof For notational simplicity, we drop the superscript B . For $i = 1, 2, \dots, N$, and $s = (1 - i), (2 - i), \dots, (N - i), s \neq 0$,

$$\begin{aligned} & \text{Cov} [\text{MMD}^2(X_i, Y), \text{MMD}^2(X_{i+s}, Y)] \\ &= \text{Cov} \left[\binom{B}{2}^{-1} \sum_{l < j} h(X_{i,l}, X_{i,j}, Y_l, Y_j), \binom{B}{2}^{-1} \sum_{p < q} h(X_{i+s,p}, X_{i+s,q}, Y_p, Y_q) \right] \\ &= \binom{B}{2}^{-2} \binom{B}{2} \binom{2}{1} \binom{B-2}{2-1} \text{Cov} [h(x, x', y, y'), h(x'', x''', y, y'')] \\ & \quad + \binom{B}{2}^{-2} \binom{B}{2} \binom{2}{2} \binom{B-2}{2-2} \text{Cov} [h(x, x', y, y'), h(x'', x''', y, y')]. \end{aligned}$$

Under null distribution,

$$\begin{aligned} & \text{Cov} [h(x, x', y, y'), h(x'', x''', y, y'')] \\ &= \int h(x, x', y, y') h(x'', x''', y, y'') d\mathbb{P}(x, x', x'', x''', y, y', y'') \\ &= \int \left(\underbrace{\int h(x, x', y, y') d\mathbb{P}(x', y')}_{=0} \right) d\mathbb{P}(x) \cdot \int \left(\underbrace{\int h(x'', x''', y, y'') d\mathbb{P}(x'', y'')}_{=0} \right) d\mathbb{P}(x'') = 0. \end{aligned}$$

Above, with a slight abuse of notation, we use $d\mathbb{P}(\cdot)$ to denote the probability measure of appropriate arguments. Finally, we have:

$$\text{Cov} [\text{MMD}^2(X_i, Y), \text{MMD}^2(X_{i+s}, Y)] = \binom{B}{2}^{-1} \text{Cov} [h(x, x', y, y'), h(x'', x''', y, y')].$$

■

B.1 Variance of B -statistics.

Proof [Proof for Lemma 1] For notational simplicity, we drop the superscript B . Using results in Lemma 13 and Lemma 14, we have

$$\begin{aligned}
 \text{Var}[Z_B] &= \text{Var} \left[\frac{1}{N} \sum_{i=1}^N \text{MMD}^2(X_i, Y) \right] \\
 &= \frac{1}{N^2} \left[N \text{Var}[\text{MMD}^2(X_i, Y)] + \sum_{i \neq j} \text{Cov} [\text{MMD}^2(X_i, Y; B), \text{MMD}^2(X_j, Y)] \right] \\
 &= \binom{B}{2}^{-1} \left[\frac{1}{N} \mathbb{E}[h^2(x, x', y, y')] + \frac{N-1}{N} \text{Cov} [h(x, x', y, y'), h(x'', x''', y, y')] \right].
 \end{aligned}$$

■

Next, we introduce Lemma 15 and Lemma 16, which are useful in proving Lemma 3.

Lemma 15 (Covariance of MMD, different block sizes, same block index.) *For blocks with the same index i but with distinct block sizes, under the null hypothesis we have*

$$\text{Cov} \left[\text{MMD}^2(X_i^{(B)}, Y^{(B)}), \text{MMD}^2(X_i^{(B+v)}, Y^{(B+v)}) \right] = \binom{B \vee (B+v)}{2}^{-1} \mathbb{E}[h^2(x, x', y, y')]. \tag{36}$$

Proof Note that

$$\begin{aligned}
 &\text{Cov} \left[\text{MMD}^2(X_i^{(B)}, Y^{(B)}), \text{MMD}^2(X_i^{(B+v)}, Y^{(B+v)}) \right] \\
 &= \text{Cov} \left[\binom{B}{2}^{-1} \sum_{l < j} h(X_{i,l}, X_{i,j}, Y_l, Y_j), \binom{B+v}{2}^{-1} \sum_{p < q} h(X_{i,p}, X_{i,q}, Y_p, Y_q) \right] \\
 &= \binom{B}{2}^{-1} \binom{B+v}{2}^{-1} \text{Cov} \left[\sum_{l < j} h(X_{i,l}, X_{i,j}, Y_l, Y_j), \sum_{p < q} h(X_{i,p}, X_{i,q}, Y_p, Y_q) \right] \\
 &= \binom{B}{2}^{-1} \binom{B+v}{2}^{-1} \binom{B \wedge (B+v)}{2} \text{Var}[h(x, x', y, y')] \\
 &= \binom{B \vee (B+v)}{2}^{-1} \mathbb{E}[h^2(x, x', y, y')],
 \end{aligned}$$

where the second last equality is due to a similar argument as before to drop block indices as they are *i.i.d.* under the null. ■

Lemma 16 (Covariance of MMD, different block sizes, different block indices.)

Under the null we have

$$\text{Cov} \left[\text{MMD}^2(X_i^{(B)}, Y^{(B)}), \text{MMD}^2(X_{i+s}^{(B+v)}, Y^{(B+v)}) \right] = \binom{B \vee (B+v)}{2}^{-1} \cdot \text{Cov} [h(x, x', y, y'), h(x'', x''', y, y')].$$

Proof Note that

$$\begin{aligned} & \text{Cov} \left[\text{MMD}^2(X_i^{(B)}, Y^{(B)}), \text{MMD}^2(X_{i+s}^{(B+v)}, Y^{(B+v)}) \right] \\ &= \text{Cov} \left[\binom{B}{2}^{-1} \sum_{l < j} h(X_{i,l}^{(B)}, X_{i,j}^{(B)}, Y_l^{(B)}, Y_j^{(B)}), \binom{B+v}{2}^{-1} \sum_{p < q} h(X_{i+s,p}^{(B+v)}, X_{i+s,q}^{(B+v)}, Y_p^{(B+v)}, Y_q^{(B+v)}) \right] \\ &= \binom{B}{2}^{-1} \binom{B+v}{2}^{-1} \text{Cov} \left[\sum_{l < j} h(X_{i,l}^{(B)}, X_{i,j}^{(B)}, Y_l^{(B)}, Y_j^{(B)}), \sum_{p < q} h(X_{i+s,p}^{(B+v)}, X_{i+s,q}^{(B+v)}, Y_p^{(B+v)}, Y_q^{(B+v)}) \right] \\ &= \binom{B}{2}^{-1} \binom{B+v}{2}^{-1} \binom{B \wedge (B+v)}{2} \text{Cov} [h(x, x', y, y'), h(x'', x''', y, y')] \\ &= \binom{B \vee (B+v)}{2}^{-1} \text{Cov} [h(x, x', y, y'), h(x'', x''', y, y')], \end{aligned}$$

where the second last equality is due to a similar argument as before to drop block indices as they are *i.i.d.* under the null. ■

B.2 Covariance of offline B -statistics.

Proof [Proof of Lemma 3] For the offline case, we have that the correlation

$$r_{B, B+v} = \frac{1}{\sqrt{\text{Var}[Z_B]}} \frac{1}{\sqrt{\text{Var}[Z_{B+v}]}} \text{Cov} [Z_B, Z_{B+v}],$$

where

$$\begin{aligned} \text{Cov} (Z_B, Z_{B+v}) &= \text{Cov} \left[\frac{1}{N} \sum_{i=1}^N \text{MMD}^2(X_i^{(B)}, Y^{(B)}), \frac{1}{N} \sum_{j=1}^n \text{MMD}^2(X_j^{(B+v)}, Y^{(B+v)}) \right] \\ &= \frac{1}{N} \text{Cov} \left[\text{MMD}^2(X_i^{(B)}, Y^{(B)}), \text{MMD}^2(X_i^{(B+v)}, Y^{(B+v)}) \right] \\ &\quad + \frac{1}{N^2} \sum_{i \neq j} \text{Cov} \left[\text{MMD}^2(X_i^{(B)}, Y^{(B)}), \text{MMD}^2(X_j^{(B+v)}, Y^{(B+v)}) \right]. \end{aligned}$$

Using results from Lemma 15 and Lemma 16, we have:

$$\begin{aligned}
 \text{Cov}(Z_B, Z_{B+v}) &= \frac{1}{N} \binom{B \vee (B+v)}{2}^{-1} \mathbb{E}[h^2(x, x', y, y')] \\
 &\quad + \frac{N-1}{N} \binom{B \vee (B+v)}{2}^{-1} \text{Cov}[h(x, x', y, y'), h(x'', x''', y, y')] \\
 &= \binom{B \vee (B+v)}{2}^{-1} \left[\frac{1}{N} \mathbb{E}[h^2(x, x', y, y')] \right. \\
 &\quad \left. + \frac{N-1}{N} \text{Cov}[h(x, x', y, y'), h(x'', x''', y, y')] \right].
 \end{aligned}$$

Finally, plugging in the expressions for $\text{Var}[Z_B]$ and $\text{Var}[Z_{B+v}]$, we have (10) for the offline case.

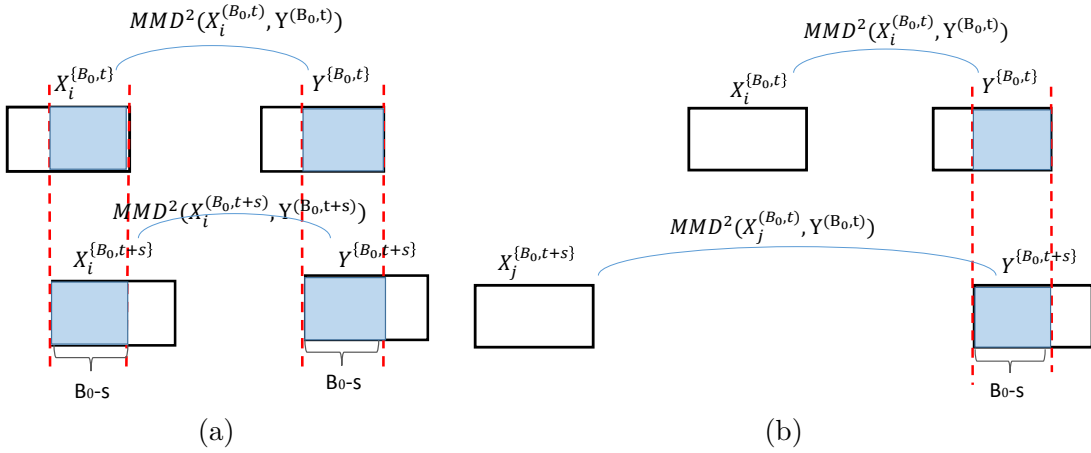


Figure 7: (a): Illustration of how $MMD^2(X_i^{\{B_0,t\}}, Y^{\{B_0,t\}})$ and $MMD^2(X_i^{\{B_0,t+s\}}, Y^{\{B_0,t+s\}})$ are constructed in the online change-point detection, where the shaded areas represent the overlapping data. Illustration of how $MMD^2(X_i^{\{B_0,t\}}, Y^{\{B_0,t\}})$ and $MMD^2(X_j^{\{B_0,t+s\}}, Y^{\{B_0,t+s\}})$, $j \neq i$ are constructed in the online change-point detection, where the shaded areas represent the overlapping data. (b): Illustration of how $MMD^2(X_i^{\{B_0,t\}}, Y^{\{B_0,t\}})$ and $MMD^2(X_j^{\{B_0,t+s\}}, Y^{\{B_0,t+s\}})$, $j \neq i$ are constructed in the online change-point detection, where the shaded areas represent the overlapping data.

B.3 Covariance of online B -statistics

Similarly, for the online case we need to analyze $r' = \text{Cov}(Z'_{B_0,t}, Z'_{B_0,t+s})$. Without loss of generality, assume $s > 0$. We adopt the same strategy as the above for a fixed block size

B_0 to obtain

$$\begin{aligned}
 & \text{Cov} \left(\text{MMD}^2(X_i^{(B_0,t)}, Y^{(B_0,t)}), \text{MMD}^2(X_i^{(B_0,t+s)}, Y^{(B_0,t+s)}) \right) \\
 = & \text{Cov} \left[\binom{B_0}{2}^{-1} \sum_{l < j}^{B_0} h(X_{i,l}^{(t)}, X_{i,j}^{(t)}, Y_l^{(t)}, Y_j^{(t)}), \binom{B_0}{2}^{-1} \sum_{p < q}^{B_0} h(X_{i,p}^{(t+s)}, X_{i,q}^{(t+s)}, Y_p^{(t+s)}, Y_q^{(t+s)}) \right] \\
 = & \binom{B_0}{2}^{-2} \binom{(B_0 - s) \vee 0}{2} \text{Var}[h(x, x', y, y')]. \tag{37}
 \end{aligned}$$

Figure 7 demonstrates how $\text{MMD}^2(X_i^{(B_0,t)}, Y^{(B_0,t)})$ and $\text{MMD}^2(X_i^{(B_0,t+s)}, Y^{(B_0,t+s)})$ are constructed. The shaded areas represent the overlapping data.

Similarly, we have

$$\begin{aligned}
 & \text{Cov} \left(\text{MMD}^2(X_i^{(B_0,t)}, Y^{(B_0,t)}), \text{MMD}^2(X_j^{(B_0,t+s)}, Y^{(B_0,t+s)}) \right) \\
 = & \text{Cov} \left[\binom{B_0}{2}^{-1} \sum_{l < k}^{B_0} h(X_{i,l}^{(t)}, X_{i,k}^{(t)}, Y_l^{(t)}, Y_k^{(t)}), \binom{B_0}{2}^{-1} \sum_{p < q}^{B_0} h(X_{j,p}^{(t+s)}, X_{j,q}^{(t+s)}, Y_p^{(t+s)}, Y_q^{(t+s)}) \right] \\
 = & \binom{B_0}{2}^{-2} \binom{(B_0 - s) \vee 0}{2} \text{Cov}(h(x, x', y, y'), h(x'', x''', y, y')), \tag{38}
 \end{aligned}$$

Figure 7 demonstrates how $\text{MMD}^2(X_i^{(B_0,t)}, Y^{(B_0,t)})$ and $\text{MMD}^2(X_j^{(B_0,t+s)}, Y^{(B_0,t+s)})$, $j \neq i$ are constructed. The shaded areas represent the overlapping data. Thus,

$$\begin{aligned}
 & \text{Cov}(Z_{B_0,t}, Z_{B_0,t+s}) \\
 = & \text{Cov} \left(\frac{1}{N} \sum_{i=1}^N \text{MMD}^2(X_i^{(B_0,t)}, Y^{(B_0,t)}), \frac{1}{N} \sum_{j=1}^N \text{MMD}^2(X_j^{(B_0,t+s)}, Y^{(B_0,t+s)}) \right) \\
 = & \binom{B_0}{2}^{-2} \binom{(B_0 - s) \vee 0}{2} \left[\frac{1}{N} \text{Var}(h(x, x', y, y')) \right. \\
 & \left. + \frac{N-1}{N} \text{Cov}(h(x, x', y, y'), h(x'', x''', y, y')) \right].
 \end{aligned}$$

Finally, plugging in the expressions for $\text{Var}[Z_{B_0,t}]$ and $\text{Var}[Z_{B_0,t+s}]$, we have (30) for the online case. \blacksquare

Appendix C. Proof of Lemma 10

Proof First, we show that the stopping time T is asymptotically exponentially distributed. The analysis of the distribution of the stopping time is based on Poisson approximation. Define an indicator of the event $\mathbf{1}_j$ such that the event $\mathbf{1}\{\max_{(j-1)m \leq t \leq jm} Z'_{B_0,t} > b\}$. Consider the time interval $[0, x]$. Note that the stopping time is not activated in the interval $[0, x]$, if and only if, all the relevant indicators are zero. For simplicity, we assume x is divisible by m . Define the random variable $\widehat{W} = \sum_{j=1}^{x/m} \mathbf{1}_j$. Hence, $\{\widehat{W} = 0\} = \{T_b > x\}$.

Thus, to find the tail probability of the stopping time, we need to show that the sum of the indicator functions converge to a Poisson distribution.

For online B -statistics, the standard Poisson limit cannot be directly applied, since the events $\{\mathbf{1}_j\}$, $j = 1, \dots, x/m$, are not independent, and we need the generalized Poisson limit theorem (Arratia et al., 1989), which allows for dependence between the variables. The setup for the theorem is as follows. Let I be an arbitrary index set, and for $\alpha \in I$, let X_α be a Bernoulli random variable with $p_\alpha = \mathbb{P}(X_\alpha = 1) > 0$. Let $W = \sum_{\alpha \in I} X_\alpha$. For each $\alpha \in I$, suppose we choose $B_\alpha \subset I$ with $\alpha \in B_\alpha$. Think of B_α as a “neighborhood of dependence” for each α , such that X_α is independent or nearly independent of all of the X_β for $\beta \notin B_\alpha$. Define $p_1 = \sum_{\alpha \in I} \sum_{\beta \in B_\alpha} p_\alpha p_\beta$, $p_2 = \sum_{\alpha \in I} \sum_{\alpha \neq \beta \in B_\alpha} \mathbb{E}(X_\alpha X_\beta)$, $p_3 = \sum_{\alpha \in I} \mathbb{E}|\mathbb{E}(X_\alpha - p_\alpha | \sigma(X_\beta : \beta \in I - B_\alpha))|$, where $\sigma(\cdot)$ represents the σ -field generated by the corresponding random field. Loosely speaking, p_1 measures the neighborhood size, p_2 measures the expected number of neighbors of a given occurrence and p_3 measures the dependence between an event and the number of occurrences outside its neighborhood. Then, we have the following

Theorem 17 (Poisson approximation, Theorem 1 in (Arratia et al., 1989)) *Let W be the number of occurrences of dependent events, and let Z be a Poisson random variable with $\mathbb{E}Z = \mathbb{E}W = \lambda > 0$. Then the total variation distance between the distributions of W and Z is bounded by*

$$\sup_{\|h\|=1} |\mathbb{E}h(W) - \mathbb{E}h(Z)| \leq p_1 + p_2 + p_3.$$

where $h : \mathbb{Z}^+ \rightarrow \mathbb{R}$, $\|h\| = \sup_{k \geq 0} |h(k)|$.

The theorem is a consequence of the powerful Chen-Stein method.

Invoking the above theorem in our online B -statistics setting, we can bound the total variation distance between the random variable, defined as the number of boundary cross events for the statistic over disjoint intervals, and a Poisson random variable with the same rate. In our setting, let $I = \{1, 2, \dots, x/m\}$ and $\mathcal{N}(j) = \{j-1, j, j+1\}$ where $j = 2, \dots, (x/m-1)$ (with obvious modifications for $j = 1$ and $j = x/m$). Then we can specify:

$$p_1 = \sum_{j \in I} \sum_{i \in \mathcal{N}(j) \setminus \{j\}} \mathbb{P}\{\mathbf{1}_j = 1\} \mathbb{P}\{\mathbf{1}_i = 1\} = 2(x/m-2)\mathbb{P}\{\mathbf{1}_1 = 1\}^2 + 2\mathbb{P}\{\mathbf{1}_1 = 1\}, \quad (39)$$

$$p_2 = \sum_{j \in I} \sum_{i \in \mathcal{N}(j) \setminus \{j\}} \mathbb{P}\{\mathbf{1}_j = 1, \mathbf{1}_i = 1\} = 2(x/m-1)\mathbb{P}\{\mathbf{1}_1 = 1, \mathbf{1}_2 = 1\}, \quad (40)$$

$$p_3 = \sum_{j \in I} \mathbb{E}\{|\mathbb{E}\{\mathbf{1}_j | \sigma\{\mathbf{1}_i : i \notin \mathcal{N}(j)\}\} - \mathbb{E}\{\mathbf{1}_j\}|\}. \quad (41)$$

We will show that p_1 , p_2 , and p_3 converge to 0 as $b \rightarrow \infty$. For p_1 , the last summand in (39) is associated with the two edge elements. It follows that p_1 is asymptotically to $(2C+2)\mathbb{P}\{\mathbf{1}_1 = 1\}$, which will converge to zero as $b \rightarrow \infty$ since $\mathbb{P}\{\mathbf{1}_1 = 1\}$ converges to zero when m is sub-exponential, i.e., $\log b \ll m \ll b^{-1}e^{\frac{1}{2}b^2}$. Next, let us examine p_2 in (40). Redefine parameter sub-region

$$S_1 = [0, m - B_0/2], \quad S_2 = [m - B_0/2, m + B_0/2], \quad S_3 = [m + B_0/2, 2m],$$

and denote Y_i , $i = 1, 2, 3$ as $\{Y_i = 1\} = \{\max_{t \in S_i} Z'_{B_0, t} > b\}$, which are the indicator functions of crossings of the threshold in the approximate sub-regions. Notice that the indicator functions Y_1 and Y_3 are independent of each other and they share the same distribution. We use the fact that unless the crossing occurs in a shared sub-region, it must simultaneously occur in two disjoint sub-regions in order to have double crossing. As a consequence, we obtain the upper bound $\mathbf{1}_1 \cdot \mathbf{1}_2 \leq Y_2 + Y_1 \cdot Y_3$, and

$$\mathbb{P}\{\mathbf{1}_1 = 1, \mathbf{1}_2 = 1\} \leq \mathbb{P}\{Y_2 = 1\} + \mathbb{P}\{Y_1 = 1\}^2 \leq \mathbb{P}\{Y_2 = 1\} + \mathbb{P}\{\mathbf{1}_1 = 1\}^2.$$

The probability $\mathbb{P}\{Y_2 = 1\}$ is proportional to $B_0 \cdot b e^{-\frac{1}{2}b^2}$. Consequently, p_2 is asymptotically bounded by $2C(B_0/m + \mathbb{P}\{\mathbf{1}_1 = 1\})$. Hence, p_2 converges to zero if $\log b \ll m \ll b^{-1}e^{\frac{1}{2}b^2}$ whenever $b \rightarrow \infty$. For p_3 in (41), $\mathbf{1}_j$ and $\mathbf{1}_i$ are computed over non-overlapping observations and are therefore independent. Thus, the term p_3 vanishes.

Next prove that the collection of stopping times $\{T_b\}$ indexed by b is *uniformly integrable*. Again consider the sequence of indicators $\{\mathbf{1}_j\}$, $j = 2k$ and $k = 1, 2, \dots$. Define the random variable τ that identifies the index of the first indicator in the sequence that obtains the value one: $\tau = \inf\{k : \mathbf{1}_{2k} = 1\}$. Note that τ has a geometric distribution. Moreover, since $T_b \leq 2m\tau$ we obtain that

$$\mathbb{P}\{T_b > x\} \leq \mathbb{P}\{\tau > x/(2m)\} = (1 - \mathbb{P}(\mathbf{1}_2 = 1))^{\lfloor x/(2m) \rfloor}.$$

The conclusion then follows from that $1/m \cdot \mathbb{P}(\mathbf{1}_2 = 1)$ converges to 0. ■

Appendix D. Dependence of EDD on block-size B_0

We investigate the dependence of EDD of the B -statistic for online change-point detection, on the pre-defined block size B_0 . This example may also shed some light on how to choose B_0 in practice. The rationale is that, on the one-hand, the expected detection delay (EDD) is greater than B_0 , since we need at least B_0 samples to compute one B -statistic. Hence, a large B_0 will artificially impose a longer EDD. On the other hand, when block size is too small, we may not pool enough post-change samples and the statistical power of the B -statistic is weak, which will also result in a large EDD. Hence, there should be an optimal choice for B_0 that minimizes the EDD. This is validated by our numerical example. Consider the distribution shifts from $\mathcal{N}(\mathbf{0}, I_{20})$ to $\mathcal{N}(\mu, I_{20})$, with μ being element-wise equal to a non-zero constant. In Figure 8(a), the shift size of the mean is 0.2, where the minimum EDD is achieved by $B_0 = 28$. Figure 8(b) shows the optimal block sizes for a range of values of the mean shift size (from 0.1 to 1.2).

We fix $B_0 = 20$ and let $x \in \mathbb{R}^{20}$. Consider a simple case where signal changes from a zero-mean Gaussian $\mathcal{N}(0, I)$ to a non-zero mean Gaussian $\mathcal{N}(\mu, I_{20})$, and the post-change mean vector μ is element-wise equal to a constant. Note when we implement this experiment, we let the mean shift change occur at the first point of the testing data. Under this scenario, the EDD would be at least B_0 , since we need at least B_0 testing samples to compute one M -statistic. In this way, we intentional get the worst case for EDD, which serve as an upper bound for the actually EDD(s) in more general sequential settings.

In Figure 8(a), we fix the Gaussian mean shift μ to be 0.2. Figure 8(a) shows the log (EDD) versus B_0 and demonstrates the tradeoff in choosing the block size for the M -statistic: when block size is too small, the statistical power of the M -statistic is weak and, hence, the EDD is large; on the other hand, when block size is too large, although statistical power is good, the EDD is also large because we have to pool a large number of samples for the post-change block which incurs a larger delay. In view of the above, there is an optimal choice for the block size, and here $B_0 = 28$ yields the smallest (EDD), which is defined as the optimal block size for a mean shift equals 0.2. Similarly, we evaluate the optimal block sizes for a range of values of the mean shift (from 0.1 to 1.2), as illustrated in Figure 8(b). In doing this, we hope to provide a guidance in how to set B_0 in practice.

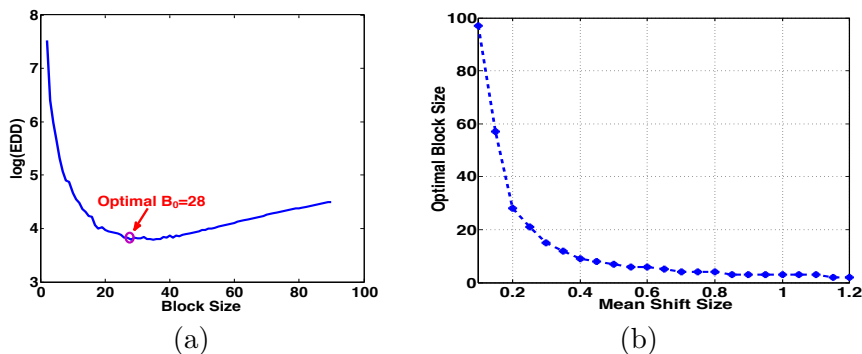


Figure 8: Online B -statistic for a case where the distribution shifts from $\mathcal{N}(\mathbf{0}, I_{20})$ to $\mathcal{N}(\mu, I_{20})$, with μ being element-wise equal to a non-zero constant. (a) $\log(\text{EDD})$ versus block size and the optimal block size $B_0 = 28$ corresponds to a minimum EDD; (b) optimal block sizes versus the size of the mean shift.

Appendix E. More details for real-data experiments

E.1 CENSREC-1-C Speech dataset

CENSREC-1-C is a real-world speech dataset in the Speech Resource Consortium (SRC) corpora provided by National Institute of Informatics (NII)⁵. This dataset contains two categories of data: (1) Simulated data. The simulated speech data are constructed by concatenating several utterances spoken by one speaker. Each concatenated sequence is then added with 7 different levels of noise from 8 different environments. So there are totally 56 different noise. Each noise setting contains 104 sequences from 52 males and 52 females speakers. (2) Recording data. The recording data is from two real-noisy environments (in university restaurant and in the vicinity of highway), and with two Signal Noise Ratio (SNR) settings (lower and higher). Ten subjects were employed for recording, and each one has four speech sequence data.

Experiment Settings. We will compare our algorithm with the baseline algorithm from (Song et al., 2013). (Song et al., 2013) only utilized 10 sequences from “STREET_SNR_HIGH”

5. Available from <http://research.nii.ac.jp/src/en/CENSREC-1-C.html>

Table 5: AUC results in CENSREC-1-C speech dataset. Simulated data are from 8 noise categories, and with two different noise levels (clean(C) and SNR 20db (S)); Recording data are from RESTAURANT_SNR_HIGH (RH), RESTAURANT_SNR_LOW (RL), STREET_SNR_HIGH (SH) and STREET_SNR_LOW (SL).

(a) Recording data

	RH	RL	SH	SL
Ours	0.7800	0.7282	0.6507	0.6865
Baseline	0.7503	0.6835	0.4329	0.6432

(b) Simulate clean data

	C1	C2	C3	C4	C5	C6	C7	C8
Ours	0.9413	0.9446	0.9236	0.9251	0.9413	0.9446	0.9236	0.9251
Baseline	0.9138	0.9262	0.8691	0.9128	0.9138	0.9216	0.8691	0.9128

(c) Simulated data with SNR=20db

	S1	S2	S3	S4	S5	S6	S7	S8
Ours	0.7048	0.7160	0.7126	0.7129	0.7094	0.7633	0.6796	0.7145
Baseline	0.7083	0.6681	0.6490	0.7119	0.6994	0.6815	0.6487	0.6541

setting in recording data. Here we will use all the settings in recording data, the SNR level 20db and clean signals from simulated data. See Figure 9 for some examples of the testing data, as well as the statistics computed by our algorithm. For each sequence, we decompose it into several segments. Each segment consists of two types of signals (noise vs speech). Given the reference data from noise, we want to detect the point where the signal changes from noise to speech.

Evaluation Metrics. We use Area Under Curve (AUC) to evaluate the computed statistics, like in (Song et al., 2013). Specifically, for each test sequence that consists of two signal distributions, we will mark the points as change-points whose statistics exceed the given threshold. If the distance between detected point and true change-point is within the size of detection window, then we consider it as True Alarm (True Positive). Otherwise it is a False Alarm (False Positive).

We use 10% of the sequences to tune the parameters of both algorithms, and use the rest 90% for reporting AUC. The kernel bandwidth is tuned in $\{0.1d_{\text{med}}, 0.5d_{\text{med}}, d_{\text{med}}, 2d_{\text{med}}, 5d_{\text{med}}\}$, where d_{med} is the median of pairwise distances of reference data. Block size is fixed to 50, and the number of blocks is simply tuned in $\{10, 20, 30\}$.

Results. Table 5 shows the AUC of two algorithms on different background settings. Our algorithm surpasses the baseline on most cases. Both algorithms are performing quite well on the simulated clean data, since the difference between speech signals and background is more significant than the noisy ones. The averaged AUC of our algorithm on all these settings is **.8014**, compared to **.7578** achieved by baseline algorithm. See the ROC curves in Figure 10 for a better comparison.

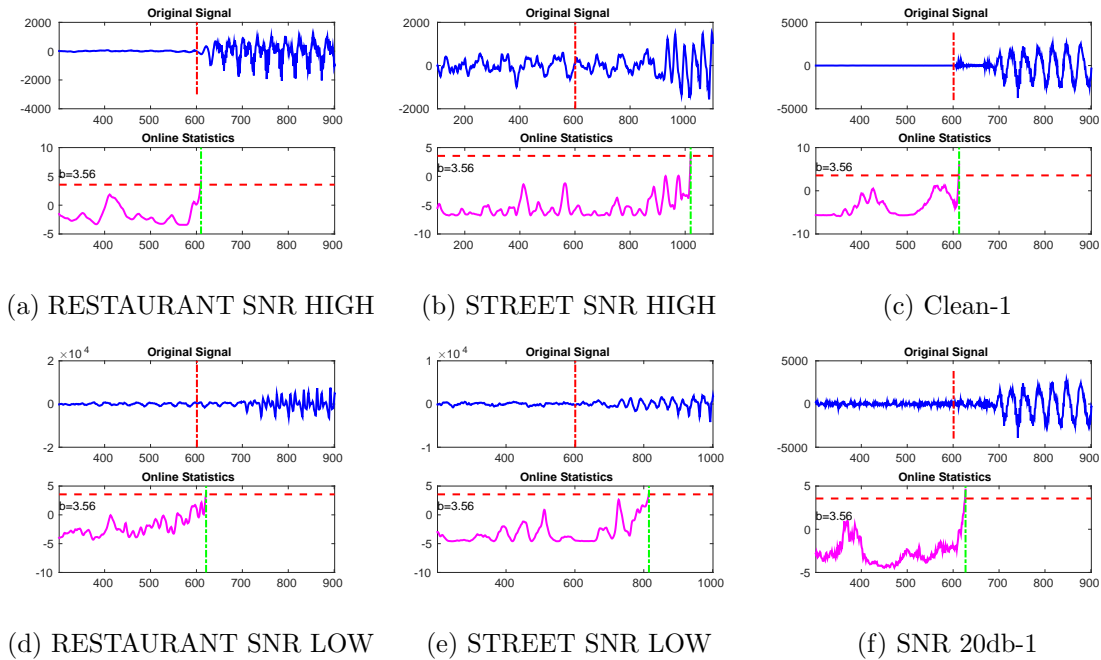


Figure 9: Examples of speech dataset. The red vertical bar shown in the upper part of each figure is the ground truth of change-point; The green vertical bar shown in the lower part is the change-point detected by our algorithm (the point where the statistic exceeds the threshold). We also plot the threshold as a red dash horizontal line in each figure. Once the statistics touch the threshold, we will stop the detection.

E.2 HASC human activity dataset

This data is from *Human Activity Sensing Consortium (HASC) challenge 2011*⁶. Each data consists of human activity information collected by portable three-axis accelerometers. Following the setting in (Song et al., 2013), we use the ℓ_2 -norm of 3-dimensional data (i.e., the magnitude of acceleration) as the signals.

We use the ‘RealWorldData’ from HASC Challenge 2011, which consists of 6 kinds of human activities:

walk/jog, stairUp/stairDown, elevatorUp/elevatorDown,
escalatorUp/escalatorDown, movingWalkway, stay.

We make pairs of signal sequences from different activity categories, and remove the sequences which are too short. We finally get 381 sequences. We tune the parameters using the same way as in CENSREC-1-C experiment. The AUC of our algorithm is **.8871**, compared to **.7161** achieved by baseline algorithm, which greatly improved the performance.

Examples of the signals are shown in Figure 11. Some sequences are easy to find the change-point, like Figure 11a, and 11d. Some pairs of the signals are hard to distinguish visually, like Figure 11b and 11c. The examples show that our algorithm can tell

6. <http://hasc.jp/hc2011>

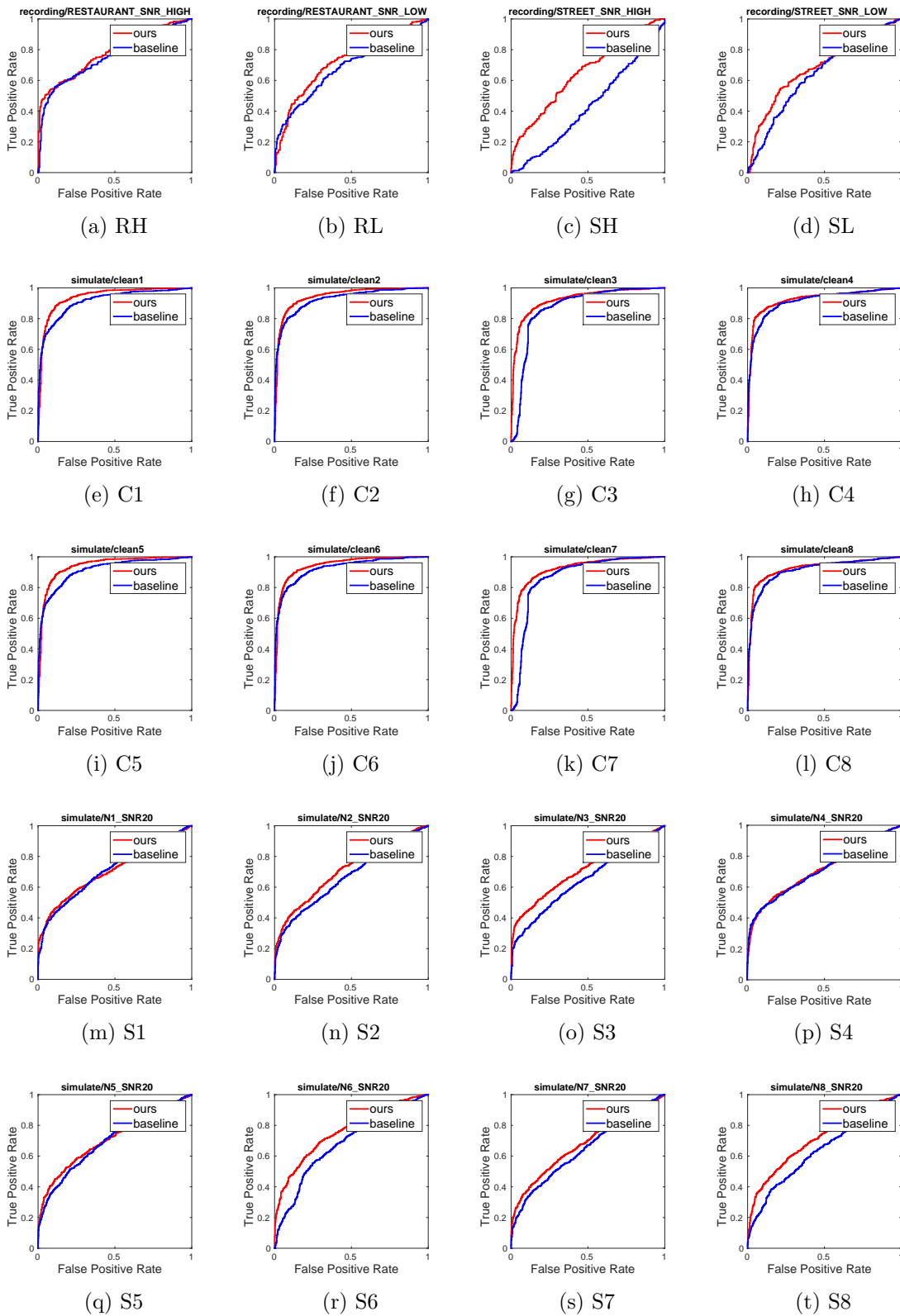


Figure 10: AUC comparison on speech dataset

the change-point from walk to stairUp/stairDown, or from stairUp/stairDown to escalatorUp/escalatorDown. There are some cases when our algorithm raises false alarm. See Figure 11h. It find a change-point during the activity ‘elevatorUp/elevatorDown’. It is reasonable, since this type of action contains the phase from acceleration to uniform motion, and the phase from uniform motion to acceleration.

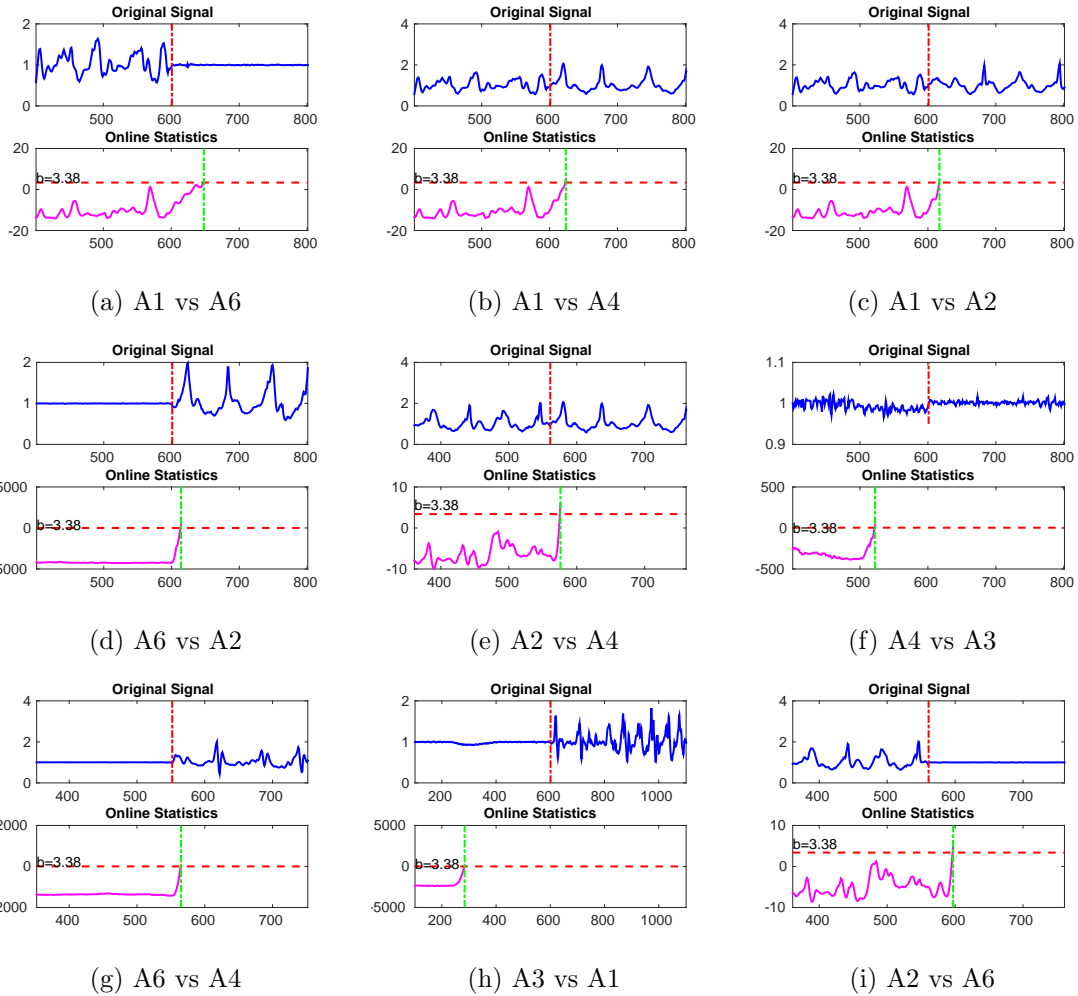


Figure 11: Examples of HASC dataset. The markers in this figure are the same as in Figure 9.

Appendix F. Skewness of B -statistics

In the following, Lemma 18, Lemma 19, and Lemma 20 are used to derive the final expression for the skewness of the statistic:

Lemma 18 *Under null hypothesis,*

$$\begin{aligned} & \mathbb{E} \left[(\text{MMD}^2(X_i, Y))^3 \right] \\ &= \frac{8(B-2)}{B^2(B-1)^2} \mathbb{E} [h(x, x', y, y')h(x', x'', y', y'')h(x'', x, y'', y)] + \frac{4}{B^2(B-1)^2} \mathbb{E} [h(x, x', y, y')^3]. \end{aligned}$$

Proof

$$\begin{aligned} \mathbb{E} \left[(\text{MMD}^2(X_i, Y))^3 \right] &= \binom{B}{2}^{-3} \mathbb{E} \left[\left(\sum_{a < b} h(X_{i,a}, X_{i,b}, Y_a, Y_b) \right)^3 \right] \\ &= \binom{B}{2}^{-3} \sum_k C_k \mathbb{E} [h_{ab}h_{cd}h_{ef}], \end{aligned}$$

where for simplicity we write $h_{ab} = h(X_{i,a}, X_{i,b}, Y_a, Y_b)$ and define C_k the corresponding number of combination under specific structure. Most of the terms in $\mathbb{E} [h_{ab}h_{cd}h_{ef}]$ vanish under the null. By enumerating all the combinations, only two terms are nonzero: $\mathbb{E} [h_{ab}h_{bc}h_{ca}]$ and $\mathbb{E} [h_{ab}h_{ab}h_{ab}]$. Then,

$$\begin{aligned} \mathbb{E} \left[(\text{MMD}^2(X_i, Y))^3 \right] &= \binom{B}{2}^{-3} \binom{B}{2} 2(B-2) \mathbb{E} [h_{ab}h_{bc}h_{ca}] + \binom{B}{2}^{-3} \binom{B}{2} \mathbb{E} [h_{ab}h_{ab}h_{ab}] \\ &= \frac{8(B-2)}{B^2(B-1)^2} \mathbb{E} [h(X_{i,a}, X_{i,b}, Y_a, Y_b)h(X_{i,b}, X_{i,c}, Y_b, Y_c)h(X_{i,c}, X_{i,a}, Y_c, Y_a)] \\ &\quad + \frac{4}{B^2(B-1)^2} \mathbb{E} [h(X_{i,a}, X_{i,b}, Y_a, Y_b)^3] \\ &= \frac{8(B-2)}{B^2(B-1)^2} \mathbb{E} [h(x, x', y, y')h(x', x'', y', y'')h(x'', x, y'', y)] + \frac{4}{B^2(B-1)^2} \mathbb{E} [h(x, x', y, y')^3]. \end{aligned}$$

■

Lemma 19 *Under null hypothesis,*

$$\begin{aligned} & \mathbb{E} \left[(\text{MMD}^2(X_i, Y))^2 \text{MMD}^2(X_j, Y) \right]_{i \neq j} \\ &= \frac{8(B-2)}{B^2(B-1)^2} \mathbb{E} [h(x, x', y, y')h(x', x'', y', y'')h(x''', x''', y'', y'')] \\ &\quad + \frac{4}{B^2(B-1)^2} \mathbb{E} [h(x, x', y, y')^2 h(x'', x''', y'', y'')]. \end{aligned}$$

Proof

$$\begin{aligned} & \mathbb{E} \left[(\text{MMD}^2(X_i, Y))^2 \text{MMD}^2(X_j, Y) \right]_{i \neq j} \\ &= \binom{B}{2}^{-3} \mathbb{E} \left[\left(\sum_{a < b} h(X_{i,a}, X_{i,b}, Y_a, Y_b) \right)^2 \left(\sum_{a < b} h(X_{j,a}, X_{j,b}, Y_a, Y_b) \right) \right] \\ &= \binom{B}{2}^{-3} \sum_k C_k \mathbb{E} [h_{i,ab}h_{i,cd}h_{j,ef}], \end{aligned}$$

where for simplicity we write $h_{i,ab} = h(X_{i,a}, X_{i,b}, Y_a, Y_b)$ and define C_k the corresponding number of combination under specific structure. Similarly, most of the terms in $\mathbb{E}[h_{i,ab}h_{i,cd}h_{j,ef}]$ vanish under the null. By enumerating all the combinations, only two terms are nonzero: $\mathbb{E}[h_{i,ab}h_{i,bc}h_{j,ca}]$ and $\mathbb{E}[h_{i,ab}h_{i,ab}h_{j,ab}]$. Then,

$$\begin{aligned}
 & \mathbb{E} \left[(\text{MMD}^2(X_i, Y))^2 \text{MMD}^2(X_j, Y) \right]_{i \neq j} \\
 &= \binom{B}{2}^{-3} \binom{B}{2} 2(B-2) \mathbb{E}[h_{i,ab}h_{i,bc}h_{j,ca}] + \binom{B}{2}^{-3} \binom{B}{2} \mathbb{E}[h_{i,ab}h_{i,ab}h_{j,ab}] \\
 &= \frac{8(B-2)}{B^2(B-1)^2} \mathbb{E}[h(X_{i,a}, X_{i,b}, Y_a, Y_b)h(X_{i,b}, X_{i,c}, Y_b, Y_c)h(X_{j,c}, X_{j,a}, Y_c, Y_a)] \\
 &\quad + \frac{4}{B^2(B-1)^2} \mathbb{E}[h(X_{i,a}, X_{i,b}, Y_a, Y_b)^2 h(X_{j,a}, X_{j,b}, Y_a, Y_b)] \\
 &= \frac{8(B-2)}{B^2(B-1)^2} \mathbb{E}[h(x, x', y, y')h(x', x'', y', y'')h(x''', x''', y'', y)] \\
 &\quad + \frac{4}{B^2(B-1)^2} \mathbb{E}[h(x, x', y, y')^2 h(x'', x''', y, y')].
 \end{aligned}$$

■

Lemma 20 *Under null hypothesis,*

$$\begin{aligned}
 & \mathbb{E} [\text{MMD}^2(X_i, Y)\text{MMD}^2(X_j, Y)\text{MMD}^2(X_r, Y)]_{i \neq j \neq r} \\
 &= \frac{8(B-2)}{B^2(B-1)^2} \mathbb{E}[h(x, x', y, y')h(x'', x''', y', y'')h(x''', x''', y'', y)] \\
 &\quad + \frac{4}{B^2(B-1)^2} \mathbb{E}[h(x, x', y, y')h(x'', x''', y, y')h(x''', x''', y'', y')].
 \end{aligned}$$

Proof Note that

$$\begin{aligned}
 & \mathbb{E} [\text{MMD}^2(X_i, Y)\text{MMD}^2(X_j, Y)\text{MMD}^2(X_r, Y)]_{i \neq j \neq r} \\
 &= \binom{B}{2}^{-3} \mathbb{E} \left[\left(\sum_{a < b} h(X_{i,a}, X_{i,b}, Y_a, Y_b) \right) \left(\sum_{c < d} h(X_{j,c}, X_{j,d}, Y_c, Y_d) \right) \left(\sum_{e < f} h(X_{r,e}, X_{r,f}, Y_e, Y_f) \right) \right] \\
 &= \binom{B}{2}^{-3} \sum_k C_k \mathbb{E}[h_{i,ab}h_{j,cd}h_{r,ef}].
 \end{aligned}$$

Similarly, most of the terms in $\mathbb{E}[h_{i,ab}h_{j,cd}h_{r,ef}]$ vanish under the null. By enumerating all the combinations, only two terms are nonzero: $\mathbb{E}[h_{i,ab}h_{j,bc}h_{r,ca}]$ and $\mathbb{E}[h_{i,ab}h_{j,ab}h_{r,ab}]$.

Then,

$$\begin{aligned}
 & \mathbb{E} [\text{MMD}^2(X_i, Y)\text{MMD}^2(X_j, Y)\text{MMD}^2(X_r, Y)]_{i \neq j \neq r} \\
 &= \binom{B}{2}^{-3} \binom{B}{2} 2(B-2) \mathbb{E} [h_{i,ab} h_{j,bc} h_{r,ca}] + \binom{B}{2}^{-3} \binom{B}{2} \mathbb{E} [h_{i,ab} h_{j,ab} h_{r,ab}] \\
 &= \frac{8(B-2)}{B^2(B-1)^2} \mathbb{E} [h(X_{i,a}, X_{i,b}, Y_a, Y_b) h(X_{j,b}, X_{j,c}, Y_b, Y_c) h(X_{r,c}, X_{r,a}, Y_c, Y_a)] \\
 &\quad + \frac{4}{B^2(B-1)^2} \mathbb{E} [h(X_{i,a}, X_{i,b}, Y_a, Y_b) h(X_{j,a}, X_{j,b}, Y_a, Y_b) h(X_{r,a}, X_{r,b}, Y_a, Y_b)] \\
 &= \frac{8(B-2)}{B^2(B-1)^2} \mathbb{E} [h(x, x', y, y') h(x'', x''', y', y'') h(x''', x''''', y'', y)] \\
 &\quad + \frac{4}{B^2(B-1)^2} \mathbb{E} [h(x, x', y, y') h(x'', x''', y, y') h(x''', x''''', y, y')].
 \end{aligned}$$

■

Proof We can write the raw third-order moment as

$$\begin{aligned}
 \mathbb{E}[Z_B^3] &= \mathbb{E} \left[\left(\frac{1}{N} \sum_{i=1}^N \text{MMD}^2(X_i, Y) \right)^3 \right] \\
 &= \frac{1}{N^3} \mathbb{E} \left[\left(\sum_{i=1}^N \text{MMD}^2(X_i, Y) \right) \left(\sum_{j=1}^N \text{MMD}^2(X_j, Y) \right) \left(\sum_{r=1}^N \text{MMD}^2(X_r, Y) \right) \right] \\
 &= \frac{1}{N^3} N \mathbb{E} [(\text{MMD}^2(X_i, Y))^3] + \frac{1}{N^3} \binom{3}{2} \binom{N}{1} \binom{N-1}{1} \mathbb{E} [(\text{MMD}^2(X_i, Y))^2 \text{MMD}^2(X_j, Y)]_{i \neq j} \\
 &\quad + \frac{1}{N^3} \binom{N}{1} \binom{N-1}{1} \binom{N-2}{1} \mathbb{E} [\text{MMD}^2(X_i, Y) \text{MMD}^2(X_j, Y) \text{MMD}^2(X_r, Y)]_{i \neq j \neq r} \\
 &= \frac{1}{N^2} \mathbb{E} [(\text{MMD}^2(X_i, Y))^3] + \frac{3(N-1)}{N^2} \mathbb{E} [(\text{MMD}^2(X_i, Y))^2 \text{MMD}^2(X_j, Y)]_{i \neq j} \\
 &\quad + \frac{(N-1)(N-2)}{N^2} \mathbb{E} [\text{MMD}^2(X_i, Y) \text{MMD}^2(X_j, Y) \text{MMD}^2(X_r, Y)]_{i \neq j \neq r} \\
 &= \frac{1}{N^2} \left\{ \frac{8(B-2)}{B^2(B-1)^2} \mathbb{E} [h(x, x', y, y') h(x', x'', y', y'') h(x'', x, y'', y)] + \frac{4}{B^2(B-1)^2} \mathbb{E} [h(x, x', y, y')^3] \right\} \\
 &\quad + \frac{3(N-1)}{N^2} \left\{ \frac{8(B-2)}{B^2(B-1)^2} \mathbb{E} [h(x, x', y, y') h(x', x'', y', y'') h(x''', x''''', y'', y)] \right. \\
 &\quad \left. + \frac{4}{B^2(B-1)^2} \mathbb{E} [h(x, x', y, y')^2 h(x'', x''', y, y')] \right\} \\
 &\quad + \frac{(N-1)(N-2)}{N^2} \left\{ \frac{8(B-2)}{B^2(B-1)^2} \mathbb{E} [h(x, x', y, y') h(x'', x''', y', y'') h(x''', x''''', y'', y)] \right. \\
 &\quad \left. + \frac{4}{B^2(B-1)^2} \mathbb{E} [h(x, x', y, y') h(x'', x''', y, y') h(x''', x''''', y, y')] \right\}
 \end{aligned}$$

$$\begin{aligned}
 &= \frac{8(B-2)}{B^2(B-1)^2} \left\{ \frac{1}{N^2} \mathbb{E} [h(x, x', y, y')h(x', x'', y', y'')h(x'', x, y'', y)] \right. \\
 &\quad + \frac{3(N-1)}{N^2} \mathbb{E} [h(x, x', y, y')h(x', x'', y', y'')h(x''', x'''' , y'', y)] \\
 &\quad \left. + \frac{(N-1)(N-2)}{N^2} \mathbb{E} [h(x, x', y, y')h(x'', x''', y', y'')h(x'''' , x''''', y'', y)] \right\} \\
 &+ \frac{4}{B^2(B-1)^2} \left\{ \frac{1}{N^2} \mathbb{E} [h(x, x', y, y')^3] \right. \\
 &\quad + \frac{3(N-1)}{N^2} \mathbb{E} [h(x, x', y, y')^2h(x'', x''', y, y')] \\
 &\quad \left. + \frac{(N-1)(N-2)}{N^2} \mathbb{E} [h(x, x', y, y')h(x'', x''', y, y')h(x'''' , x''''', y, y')] \right\}.
 \end{aligned}$$

■

Appendix G. Argument that Z_B does not converge to Gaussian

Note that the third-order moment of Z_B scales as $\mathcal{O}(B^{-3})$ (due to (33)), but when dividing by its variance which scales as $\mathcal{O}(B^{-2})$, the skewness becomes a constant with respect to B . Furthermore, examining the Taylor expansion of moment generating function at $\theta = 0$, we have

$$\mathbb{E}[e^{\theta Z'_B}] = 1 + \underbrace{\mathbb{E}[Z'_B]}_0 \theta + \frac{\theta^2}{2} \underbrace{\mathbb{E}[(Z'_B)^2]}_1 + \frac{\theta^3}{6} \mathbb{E}[(Z'_B)^3 e^{\theta Z'_B}] + o(\theta^3).$$

Recall that the moment generating function of a standard normal Z is given by $\mathbb{E}[e^{\theta Z}] = 1 + \theta^2/2 + o(\theta^3)$. The difference between the two moment generating functions is given by

$$\left| \mathbb{E}[e^{\theta Z'_B}] - \mathbb{E}[e^{\theta Z}] \right| = \frac{|\theta|^3}{6} |\mathbb{E}[(Z'_B)^3 e^{\theta' Z'_B}]| + o(\theta^3) > \frac{|\theta|^3}{6} c |\mathbb{E}[(Z'_B)^3]| + o(\theta^3), \quad (42)$$

where the inequality is due to the fact that $e^{\theta' Z'_B} > 0$ and we may assume it is larger than an absolute constant c . Note that the first term on the right hand side of (42) is given by $(c\theta^3/6)\text{Var}[Z_B]^{-3/2}|\mathbb{E}[Z_B^3]|$, which is clearly bounded away from zero. Hence,

$$\left| \mathbb{E}[e^{\theta Z'_B}] - \left(1 + \frac{\theta^2}{2}\right) \right| > \frac{|\theta|^3}{6} \gamma + o(\theta^3)$$

for some constant $\gamma > 0$. This shows that the difference between the moment generating functions of Z'_B and a standard normal is always non-zero and, hence, Z'_B does not converge to a standard normal in any sense.